Electrical Power and Energy Systems 147 (2023) 108770

Contents lists available at ScienceDirect

International Journal of Electrical Power and Energy Systems

journal homepage: www.elsevier.com/locate/ijepes

An optimal real-time pricing strategy for aggregating distributed generation and battery storage systems in energy communities: A stochastic bilevel optimization approach

Seyedfarzad Sarfarazi [a,*,1], Saeed Mohammadi [b,2], Dina Khastieva [b], Mohammad Reza Hesamzadeh [b], Valentin Bertsch [c], Derek Bunn [d]

[a] German Aerospace Center (DLR), Stuttgart, Germany
[b] KTH Royal Institute of Technology, Stockholm, Sweden
[c] Ruhr University Bochum, Bochum, Germany
[d] London Business School, London, United Kingdom

ARTICLE INFO

Keywords:
Battery storage system
Bilevel optimization
Branch and bound
Demand response
Energy community
Real-time pricing

ABSTRACT

The expansion of distributed electricity generation and the increasing capacity of installed battery storage systems at the community level have posed challenges to efficient technical and economic operation of the power systems. With advances in smart-grid infrastructure, many innovative demand response business models have sought to tackle these challenges, while creating financial benefits for the participating actors. In this context, we propose an optimal real-time pricing (ORTP) approach for the aggregation of distributed energy resources within energy communities. We formulate the interaction between a community-owned profit-maximizing aggregator and the users (consumers with electricity generation and storage potential, known as "prosumagers", and electric vehicles) as a stochastic bilevel disjunctive program. To solve the problem efficiently, we offer a novel solution algorithm, which applies a linear quasi-relaxation approach and an innovative dynamic partitioning technique. We introduce benchmark tariffs and solution algorithms and assess the performance of the proposed pricing strategy and solution algorithm in four case studies. Our results show that the ORTP strategy increases community welfare while providing useful grid services. Furthermore, our findings reveal the superior computational efficiency of our proposed solution algorithm in comparison to benchmark algorithms.

1. Introduction

1.1. Motivation

The lower levelized cost of electricity from photovoltaic (PV) systems compared to residential retail tariffs has incentivized households in many countries to invest in rooftop PV systems [2]. Similarly, developments in battery storage systems (BSSs) are making them economically viable for use by electricity consumers. Thus, a combination of home energy storage (HES) and rooftop PV systems has been shown to be profitable under various regulatory schemes, leading to the emergence of so-called "prosumagers" (consumers with electricity generation and storage potential[3]) as new market actors [3]. Furthermore, improved charging infrastructures and policy support measures have made electric vehicles (EVs) more competitive for mobility and introduced them into the mix of distributed energy resources (DERs) [4]. However, this growth of DERs poses significant challenges for the electricity system; For economic efficiency, end-user activities should be aligned with market signals [5] and provide system benefits [6].

With the expansion of smart-grid infrastructure, several innovative demand response (DR) business models are seeking to meet these challenges. Ideally, the focus of these business models should be the

* Corresponding author.
E-mail address: Seyedfarzad.sarfarazi@dlr.de (S. Sarfarazi).

[1] This research is financed by the German Aerospace Center (DLR) basic-funding project SoGuR.

[2] This work was financially supported by the Swedish Energy Agency (Energimyndigheten) under Grant 3233. The required computation is performed by computing resources from the Swedish National Infrastructure for Computing (SNIC) at PDC center for high performance computing at KTH Royal Institute of Technology which was supported by the Swedish Research Council under Grant 2018-05973.

[3] In this paper, we adopt the naming convention suggested in [1] and refer to an electricity consumer with generation potential as a prosumer (producer and consumer). A prosumager additionally operates an energy storage system to increase self-consumption (producer, consumer and storage).

https://doi.org/10.1016/j.ijepes.2022.108770
Received 1 June 2022; Received in revised form 8 October 2022; Accepted 31 October 2022
Available online 1 December 2022

Nomenclature

Parameters

Γ^{S}, Γ^{B}	Aggregator's sale and purchase margin in benchmark tariffs
θ_i^{B}	Battery capacity of user i
M^{B}, M^{S}	Sufficiently large constants
P_i^{Q}	Marginal operational cost of charging/discharging the BSS for user i
η_i^{C}, η_i^{D}	Battery charge and discharge efficiencies for user i
$\overline{W}_t$	Maximum available line capacity behind the PCC in t
CW	Community welfare
C'	Total cost of all users
G_{itv}, L_{itv}	Electricity generation and load of user i in v and t
N	Last discrete step
P_{tv}^{M}	Wholesale electricity market price in t and v
$\overline{Z}_i^{C}, \overline{Z}_i^{D}$	Battery charge and discharge power limits for user i
$\overline{G}_i, \overline{L}_i$	Nominal power limits for user i
$\underline{P}^{B}, \overline{P}^{B}$	Aggregator's purchase price limits
$\underline{P}^{S}, \overline{P}^{S}$	Aggregator's sale price limits
μ_c, σ_c	Mean value and standard deviation of data in cluster c
$\overline{T}$	Last optimization step
C_{iv}	Cost of user i in v
P^{S}, P^{B}	Aggregator's discrete sale and purchase prices
ϕ_v	Probability of scenario v
Λ_i	Battery self-discharge rate for user i
U_{it}	Battery availability of user i in t
$\underline{A}_i, \overline{A}_i$	Battery state of charge limits for user i
$\underline{H}_t^{X}, \underline{H}_t^{X}, \underline{p}_t^{X\star}, \overline{p}_t^{X\star}$	Intermediary parameters of the MBB algorithm in t
S^{X}	Size of each discrete step in the MBB algorithm
LB	Problem's lower bound in the MBB algorithm

Sets

χ	Set of user's decision variables in (1)
ξ	Set of decision variables in (9)
ϱ	Set of decision variables in (15)
$\mathcal{C}$	Set of clusters in k-method
Υ	Set of user-specific model parameters

Indices

c	Cluster in the scenario generation algorithm
k	Discretization step
X	Trade direction: Sale or purchase in t
t	Optimization time
v	Scenario index
i	User index

Variables

r	Aggregator's total profit
r_{itv}	Aggregator's profit considering user i in v and t
$\alpha, \beta, \lambda, \gamma, \tau, \upsilon, \mu$	Lagrangian dual variables
ψ_{itv}	Binary variable for user i to avoid simultaneous charge and discharge in v and t
b_{tvk}^{S}, b_{tvk}^{B}	Binary variables in the MILP formulation for t, v and k
z_{itv}^{C}, z_{itv}^{D}	Charged and discharged power for user i in v and t
h_{itkv}^{X}	Continuous variables in the MILP formulation
d_t^{B}, d_t^{S}	Spanning variables in t
$\pi_{itv}^{S}, \pi_{itv}^{B}$	Bilinear terms after single level reduction for user i in v and t
c_{itv}	Cost of user i in v and t
e_{itv}^{S}, e_{itv}^{B}	Grid usage and feed-in of the user i in t and v
$e_{itv}^{S(0)}, e_{itv}^{S(1)}, e_{itv}^{B(0)}, e_{itv}^{B(1)}$	Non-negative intermediary variables in the quasi-relaxed formulation for user i in v and t
p_t^{S}, p_t^{B}	Aggregator's sale and purchase prices
s	Silhouette value in the k-mean clustering method
a_{itv}	Battery state of charge for user i in t and v
$\underline{p}_t^{X}, \overline{p}_t^{X}$	Dynamic lower and upper bounds of aggregator sale prices in t

provision of incentives that are compatible with the needs of the system. The most common DR schemes instruct consumers to change their consumption patterns upon request or according to a contractual agreement [7]. However, a lack of customer privacy and system scalability are major drawbacks of these directive approaches [8]. Alternatively, in price-based schemes, consumers are exposed to time-varying prices that reflect the cost of electricity and grid conditions. Furthermore, these price-based schemes do not suffer from the same privacy and scalability issues [7]. Real-time pricing (RTP) is perhaps the best-known example of this approach [9]. Although RTP can increase the alignment of BSS dispatch with wholesale market signals [5], it does not usually reflect the local level of generation and the constraints of the grid; achieving this requires more comprehensively specified optimal real-time pricing (ORTP).

This paper considers an energy community (EC) that is not isolated from the wholesale market and is managed by a community-owned aggregator (real-world examples of such ECs can be found in [10] and [11]). We have developed a methodology for the aggregator to set ORTP and show how this can improve the EC's welfare in comparison to an RTP strategy. The economic profitability of ORTP is subjected to many uncertainties associated with wholesale electricity prices as well as the power demand and supply. Therefore, such local aggregators operate under conditions of bounded rationality. Therefore, we also provide a solution for the aggregator to deal with its limited knowledge regarding the market prices, the level of local power generation, and users' electricity demands.

In the remainder of this section, we provide an overview of the background research in this context and thereby identify the research gap to which we contribute.

Table 1
Drawbacks of the reviewed single-level DR studies compared to the chosen bilevel approach.

Approach	Examples	Focus	Drawbacks
Single user optimization	[15,16,24]	Detailed modeling of the user-side reaction to dynamic prices	• Lack of energy-sharing potential • Ignores the aggregator-side strategy
User coordination	[17]	Coordination of multiple users in reaction to external prices	• Interests of the higher-level actors are neglected
Local power markets	[20–22]	Distributed trading of electricity	• Internal prices do not reflect the state of the larger energy system
Retailer-side strategy	[12–14]	Creating dynamic prices for users	• Simplified modeling of the user-side strategy • Internal prices do not reflect the state of DERs

1.2. Background research and contributions

The contributions of this paper can be broadly embedded into two bodies of literature: On the one hand, we contribute to the research area of modeling price-based DR measures for end users in energy communities. In Section 1.2.1, we provide an overview of relevant publications and highlight the novelties of our proposed model. On the other hand, our methodology contributes by proposing a relaxation technique and an algorithm to solve the resulting bilevel optimization problem. In Section 1.2.2, we review the common approaches to solving the bilevel problems that emerge in modeling the hierarchical interactions between an aggregator and users and show the advantages of our proposed approach.

We summarize contributions of this paper in Section 1.2.3.

1.2.1. Price-based DR in energy communities

Residential DR programs in the context of the smart-grid have been extensively studied in recent years [7,9]. A significant fraction of this body of literature has examined efficient dynamic pricing strategies for electricity consumers [12]. Considering consumer adoption barriers, the authors of [13] designed and analyzed dynamic tariffs that can provide considerable cost savings for households. Similarly, the authors of [14] proposed a day-ahead and real-time pricing strategy for a smart-home community to benefit the consumers while reducing their power peak-to-average ratio.

A growing body of literature has focused on the demand-side implementation of DR measures and studied optimization strategies for individual users. For example, the authors of [15] proposed a scheduling optimization model for smart-home appliances to reduce the peak load value and electricity cost. The price-based DR presented in [16] is implemented through control algorithms for different types residential consumer appliances. With a broader perspective, the authors of [17] suggested an autonomous and distributed demand-side energy-management system for efficient coordination of multiple users in reaction to external dynamic prices. The demand-side management design in [18] includes a group of passive consumers and active users with DERs.

DR has also been studied in the context of peer-to-peer markets with little or no interaction with a central energy system [19]. For example, in [20] a two-stage energy sharing strategy for a building cluster with distributed transaction was proposed. Considering a similar setup, buildings in [21] can directly share their energy supplies and demands within the community. The authors of [22] used an agent-based model to study the implementation of DR measures in a local energy market that is not isolated from the public grid.

Although all the works noted above offer beneficial features for both the users and the grid, they generally fail to take the (often conflicting) interests of the actors of the higher-level energy system (e.g., retailers) into account. In this regard, the hierarchical nature of different decision levels can be captured using bilevel optimization models [23]. Table 1 summarizes the reviewed single-level solutions and compares them with the bilevel approach chosen in this work.

There is an extensive body of research that applies game-theoretic frameworks or bilevel optimization models, in which the users follow the pricing strategy of the aggregator [25,26]. However, many of the existing models do not consider the load-shifting potential that results from storage systems such as BSSs. For example, in an uncertain environment, the EV aggregator in [27] offers selling prices to the EV owners. In a similar setup, the decision-making variables of the DR clients in [28] choose the most competitive aggregator. Without load-shifting potential, the EV owners switch to rival aggregators to minimize their energy procurement costs. In other models, users must adapt their preferred electricity demand under strong pricing incentives. For example, in the models of [29] and Yu and Hong [30], users adjust the amount of electricity they consume based on a satisfaction function. In the time-and-level-of-use scheme studied in [31], consumers must book an energy capacity within each optimization time frame. In the pricing process, the electricity consumption of the consumers is unknown to both the supplier and the consumer themselves. The proposed two-stage optimization model presented in [32] consists of a real-time optimization stage, in which the microgrid operator generates separate buy and sell RTPs, and the prosumers decide on the amount of their hourly electricity consumption. Alternatively, in our context, because users may own a BSS, they are not required to reshape their desired demand profiles.

Among the studies that have considered load-shifting with BSSs, in the model of [33] a competitive community energy storage (CES) operator trades with the grid and offers RTP to trade with users. The users in this model decide on the electricity they trade with the grid and the CES operator. From a social planner's perspective, the retailer in [34] interacts with a CES operator and provides RTP for users to minimize their total costs. In these studies, user-owned energy storage systems are neglected. The aggregator in [35] also operates a CES and can adopt either a profit-maximizing or self-sufficiency-maximizing strategy. With full knowledge of market prices, electricity generation, and power demand, the aggregator generates buy and sell RTPs for the users in the EC to elicit a desired load and feed-in pattern. The presented model of the interplay between users with BSSs and a social-welfare-optimizing aggregator in [36] can be effectively used to size the EC. The aggregator agent in [37] provides sale prices for self-optimizing EVs for optimal bidding in the day-ahead reserve market.

None of the above formulations have considered uncertain input parameters, and do not include a more generally applicable scenario-generation algorithm. In our bilevel optimization model, we take these three sources of uncertainty into account. The stochastic bilevel framework presented in [28,38] determines the optimal involvement in the wholesale market and its trading with the wind-generation units while anticipating the reaction of the EVs and responsive loads. The authors of this work showed that the implemented regret-based bidding strategy is effective for hedging the risks of uncertainties. However, the presented model, unlike our model, does not consider bilateral trading with the clients and does not take prosumagers into account. Herein, we take the EC grid restrictions into account and include a novel scenario-generation approach for stochastic optimization. Table 2 compares the existing bilevel models in comparison to our model.

Table 2
Comparative overview of the bilevel RTP models in the literature.

Papers	BSS optimization	User-owned BSS	Prosumager	EV	EC grid restrictions	Bi-directional trading	Uncertain parameters
[29,30,39–43]	✗	✗	✗	✗	✗	✗	✗
[31]	✗	✗	✗	✗	✗	✗	✓
[32–34,44,45]	✓	✗	✗	✗	✗	✗	✗
[28]	✗	✗	✗	✗	✗	✗	✓
[27]	✗	✗	✗	✓	✗	✗	✓
[38]	✓	✓	✗	✓	✗	✗	✓
[36]	✓	✓	✓	✗	✗	✓	✗
[37]	✓	✓	✗	✓	✗	✗	✗
[46]	✓	✓	✗	✗	✗	✗	✗
[35]	✓	✓	✓	✗	✗	✓	✗
This paper	✓	✓	✓	✓	✓	✓	✓

1.2.2. Solution to DR bilevel problems

Bilevel optimization is widely used to solve consumer's DR problems arising in the power sector [23]. Bilevel problems are generally hard to solve; even linear bilevel problems are shown to be NP-hard problems [47]. Different approaches have been used to solve bilevel optimization problems in the literature.

Several studies have used heuristics algorithms [48]. For example, the bilevel problem in the modeled energy-sharing solution in [49] is solved with a closed-loop iterative algorithm based on the Brouwer fixed-point-theorem. Moreover, the authors of [35,42,43,50] used genetic algorithms to iterate between the upper- and lower-level problems and search for the optimal solution. However, heuristic algorithms have the drawback that they cannot guarantee that the global solution is actually found [51].

If the lower-level problem is modeled as a differentiable function, one can derive the optimal solution mathematically and replace it in the upper-level problem. This leads to a single-level problem, which is solvable using commercial solvers. This approach has been used extensively in the context of DR modeling. For example, in [29,32,41] the utility of consumers is modeled in a logarithmic relationship with consumed energy. To model the objectives of the users, the authors of [33,34,44,46] employed quadratic cost functions as strictly convex and increasing functions of demand. Although this method can be used to solve bilevel problems to their global optimum in an efficient manner, the required underlying assumptions for the problem formulation make it impractical for many real-world applications [35].

Another common approach to solving bilevel problems is using mathematical techniques such as the Karush–Kuhn–Tucker (KKT) optimality conditions to transform the problem into an equivalent mathematical program with equilibrium constraints that is solvable with commercial solvers [52]. Under certain conditions, the emerging complementary slackness constraints can be replaced by the strong duality condition to eliminate the bilinear terms. These two approaches for single-level reduction are employed in [53] to solve the microgrid investment and operation planning bilevel problem. Among the literature reviewed in Section 1.2.1, the authors of [27,28,36,38] used this methodology. In many cases, the resulting single-level problem contains many binary variables and requires a high computational effort to solve [54]. In this paper, we propose a quasi-relaxation technique and an innovative solution algorithm to eliminate the binary variables that appear in the single-level reduction process and correspondingly solve the problem efficiently.

1.2.3. Contributions

Against this background, this paper makes the following research contributions:

1. We propose a bilevel stochastic nonlinear programming model to find the buy–sell ORTP for a community-owned profit-maximizing aggregator that manages for users (including prosumagers and EVs) in a smart EC. We show that the profit-maximizing operation also maximizes the welfare of the EC. In two transformation steps, we derive a stochastic disjunctive program from the original bilevel stochastic nonlinear program. To enable this transformation, we first apply a single-level reduction technique using KKT optimality and strong duality conditions and then discretize the aggregator's prices. We use a multi-parameter cluster-based (MPCB) scenario-generation approach to produce the required representative scenarios for the key uncertainties in the stochastic optimization problem.
2. We provide an efficient solution to the reformulated disjunctive program. We apply a linear quasi-relaxation approach to eliminate the nonlinear terms and propose a novel modified branch-and-bound (MBB) algorithm that imposes the relaxed constraint. Moreover, we extend the algorithm used in [54] and [55] by employing a dynamic partitioning approach, which disentangles the optimization results from the disjunctive parameters and reduces the computational effort needed to solve the problem.
3. We present a comprehensive analysis, regarding the effectiveness of the proposed ORTP scheme and solution algorithm. For this analysis, we compare the ORTP tariff with two benchmark tariffs: average pricing and RTP. Moreover, we demonstrate the superior computational performance of the proposed MBB algorithm in comparison with the branch-and-bound algorithm suggested in [54] and a standard mixed-integer linear programming (MILP) formulation that is used extensively in the literature. We parameterize the model with real data, examine several case studies, and evaluate the effectiveness of the proposed ORTP strategy against two benchmark tariffs.

The remainder of this paper is organized as follows. The methodology is described in Section 2, where we present our EC model and the proposed bilevel problem. In this section, we reformulate the mathematical problem into a quasi-relaxed stochastic disjunctive program and describe the developed MBB algorithm to solve the resulting problem. Section 2 also contains the definitions of the benchmark models and tariffs used to assess the results as well as a description of the data used in our analysis. This section ends with the explanation of the developed MPCB scenario-generation algorithm and the used data in the case studies. In Section 3, we introduce four case studies and demonstrate the performance of the ORTP tariff and the MBB algorithm. In Section 4, we compare the results of the case studies with those of the benchmark cases. The limitations of our methodology and the transferability of our results to real-world cases are critically discussed in 5. Section 6 concludes.

2. Methodology

2.1. Model structure

ECs represent multifaceted sociotechnical systems that, depending on their context and purpose, can have numerous definitions and diverse forms [56]. The bottom-up model developed in this work adopts the following definition: *"An EC is a group of electricity users (whether with or without DERs) that are connected to the same distribution network. Each user is metered separately and operates under a contract with a community-owned aggregator. The aggregator manages the electricity*

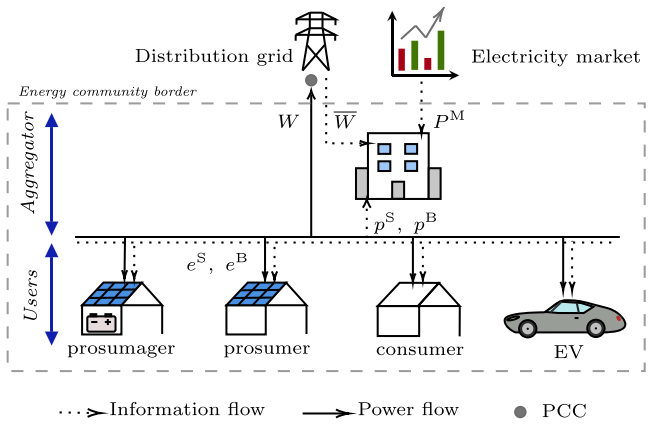

Fig. 1. Schematic illustration of the modeled energy community.

demand and generation of the EC by trading within the community and in the electricity market". Note that in our definition, we do not consider the possibility of collective self-consumption or virtual sharing of the electricity in the EC. The EC modeled according to this definition is schematically illustrated in Fig. 1.

The EC aggregator is an agent that maximizes its profit (r) by optimizing its hourly trading in the day-ahead electricity market (henceforth referred to as the market) and with the users in the EC, while considering the predicted EC grid limitations over the next day. For this optimization, the aggregator receives a forecast of the upcoming market prices (P^M) and the maximum available line capacity behind the point of common coupling (PCC) ($\overline{W}_t$). It also sets the real-time sell and buy prices (p^S, p^B) to trade with the users within the community. To isolate the effects of the ORTP, we consider a case in which the aggregator does not operate a BSS. Therefore, the aggregator's demand and supply bids to the market correspond to the EC's residual load and generation, respectively.

Users within the EC can be parameterized as consumers, prosumers, prosumagers, or EVs. For the case of a prosumager, the user's model and the interaction with the aggregator is schematically shown in Fig. 2. Users with BSS optimize their interactions with the EC grid, i.e., their power consumption and feed-in (e^S, e^B) to minimize their costs (C). We assume that the users are equipped with the processing and controlling systems required for this optimization. Since the user's bidirectional grid interaction is measured with a single smart meter, the actual interaction with the grid is unidirectional in each time step ($e^S = 0$ if $e^B > 0$ and vice versa).[4] Moreover, the considered metering scheme allows a behind-the-meter consumption of the self-generated electricity. Due to the near-zero marginal cost of the rooftop PV systems, we assume that the electricity generated by the users is primarily used to cover their electricity demand. If the electricity generated by the user (G) is less than demand (L), the difference must be covered by the BSS or from the grid. Similarly, if the electricity generation exceeds the demand, the user will feed the residual generation into the BSS or sell to the grid. We also assume that the electricity consumption of the users is price inelastic, and the only source of flexibility is the load-shifting potential with the BSS. The parameter Λ_i considers the self-discharge rate, while η_i^C and η_i^D account for charge and discharge efficiency of the BSS. The state of charge (SOC) of the BSS (modeled as a) has an initial value of $\underline{A}_i$ and is limited by its lower and upper limits ($\underline{A}_i$, $\overline{A}_i$). By adding an availability factor (U_{it}), we take into account the inability

[4] Note that the metering scheme in our model differs from the gross-metering scheme, in which the electricity consumption and generation are metered separately. Furthermore, unlike net-metering schemes, the users cannot consume the electricity fed into the grid at a later time free of charge.

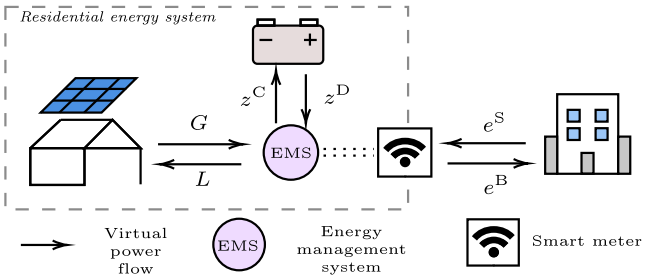

Fig. 2. Schematic overview of the prosumager's model.

or unwillingness of the users to charge their BSSs. This is particularly important in the case of EVs, as these users may not be connected to the grid during the whole day.

The interplay between the aggregator and users within this model structure leads to a hierarchical decision-making formulation, specified as a bilevel program, in which the aggregator's and users' optimizations are the upper- and lower-level problems, respectively.

2.2. Bilevel program

The stochastic bilevel programming model is formulated in (1), in which the indices i, t, and v refer to each user, optimization time, and probabilistic scenario, respectively:

$$\underset{p_t^S, p_t^B}{\text{Maximize}}\ r = \sum_{i,t,v} \phi_v \underbrace{(P_{tv}^M(e_{itv}^B - e_{itv}^S) + p_t^S e_{itv}^S - p_t^B e_{itv}^B)}_{=r_{itv}} \tag{1a}$$

$$\text{subject to: } \underline{P}^S \le p_t^S \le \overline{P}^S,\ \underline{P}^B \le p_t^B \le \overline{P}^B, \tag{1b}$$

$$-\overline{W}_t \le \sum_i (e_{itv}^S - e_{itv}^B) \le \overline{W}_t, \tag{1c}$$

$$\text{where } e_{itv}^S, e_{itv}^B \in \underset{\chi}{\text{argmin}}\ C_{iv} = \sum_t \underbrace{(p_t^S e_{itv}^S - p_t^B e_{itv}^B + P_i^Q(z_{itv}^C + z_{itv}^D))}_{=c_{itv}}, \tag{1d}$$

$$\text{subject to: } a_{itv} = \Lambda_i a_{i(t-1)v} + \frac{\eta_i^C z_{itv}^C}{\theta_i^B} - \frac{z_{itv}^D}{\eta_i^D \theta_i^B} : (\lambda_{itv}^a), \tag{1e}$$

$$z_{itv}^C = e_{itv}^S - e_{itv}^B + G_{itv} - L_{itv} + z_{itv}^D : (\lambda_{itv}^z), \tag{1f}$$

$$\underline{A}_i \le a_{itv} \le \overline{A}_i : (\underline{\tau}_{itv}, \overline{\tau}_{itv}), \tag{1g}$$

$$a_{itv} = \underline{A}_i : (\alpha_{i0v}^a), t = 0, \tag{1h}$$

$$0 \le e_{itv}^B \le \overline{G}_i : (\underline{\mu}_{itv}, \overline{\mu}_{itv}), \tag{1i}$$

$$0 \le e_{itv}^S \le \overline{L}_i : (\underline{\upsilon}_{itv}, \overline{\upsilon}_{itv}), \tag{1j}$$

$$0 \le z_{itv}^C \le U_{it}\overline{Z}_i^C \psi_{itv} : (\underline{\beta}_{itv}, \overline{\beta}_{itv}), \tag{1k}$$

$$0 \le z_{itv}^D \le U_{it}\overline{Z}_i^D (1 - \psi_{itv}) : (\underline{\gamma}_{itv}, \overline{\gamma}_{itv}). \tag{1l}$$

where χ in (1d) is the set of the user's decision variables $\chi = \{e_{itv}^S, e_{itv}^B, a_{itv}, z_{itv}^C, z_{itv}^D\}$. The symbols in parentheses (i.e., λ_{itv}^a, λ_{itv}^z, $\overline{\beta}_{itv}$, $\underline{\beta}_{itv}$, $\overline{\gamma}_{itv}$, $\underline{\gamma}_{itv}$, $\underline{\gamma}_{itv}$, $\overline{\mu}_{itv}$, $\underline{\mu}_{itv}$, $\overline{\tau}_{itv}$, $\underline{\tau}_{itv}$, α_{i0v}^a, $\overline{\upsilon}_{itv}$, and $\underline{\upsilon}_{itv}$) are the Lagrangian dual variables of the corresponding constraint in the lower-level problem. Eq. (1a) represents the utility function of the aggregator and ϕ_v is the probability of each scenario. Eq. (1b) sets bounds to ensure that the aggregator's prices in the EC are no worse than those of the public grid ($\underline{P}^S$, $\overline{P}^S$, $\underline{P}^B$, and $\overline{P}^B$ are the lower and upper limits for the aggregator's sell and buy prices). We make these assumptions in the absence of competition among different aggregators and retailers. The total power imported/exported through the line that connects the EC

to the PCC is limited in Eq. (1c), where $\overline{W}_t$[5] is the maximum available capacity of this line at time t. The user's objective in Eq. (1d) is to minimize the total operation costs for the given optimization period ($\overline{T}$). Therefore, the lower-level objective is unique for each pair of i and v. The parameter P_i^{Q} is a strictly positive value representing the marginal operation cost of the BSS. Eq. (1e) describes the SOC of the BSS, which depends on the SOC in the previous time step, the self-discharge rate (Λ_i), and the charged and discharged amount (z_{itv}^{C} and z_{itv}^{D}). The constraint in (1f) guarantees that the incoming and outgoing power flows for each user and time step are balanced. Constraint (1g) makes sure that the SOC of the BSS stays within an acceptable range. Eqs. (1i) and (1j) consider the users' nominal power constraints ($\overline{L}_i$ and $\overline{G}_i$). The battery charge and discharge in each step are limited by the maximum allowed power constraints ($\overline{Z}_i^{\mathrm{C}}$, $\overline{Z}_i^{\mathrm{D}}$), the availability of the battery, and the binary variable ψ_{itv}, which prevents simultaneous charging and discharging of the BSS. In the proposed stochastic model, the aggregator considers the uncertainty of market prices as well as the users' electricity generation and load when deciding the hourly sell and buy prices. To cope with these uncertainties and achieve the best solution, the aggregator must solve the bilevel problem for various scenarios. This means that, for a set of scenarios and for each step, a unique solution (p_t^{S} and p_t^{B}) is delivered to the users. The problem of the users also incorporates uncertainties regarding their demand and generation.

Note that the fact that the aggregator maximizes its profit does not compromise its fiduciary obligation to the EC, since the welfare of the EC is, in this case, maximized (see Proposition 1). The actual redistribution of the aggregator's profit among the EC users can be done in several ways to reflect their respective interests, but these considerations are subsidiary and outside the scope of this analysis.

Proposition 1. *Solving (1) is equivalent to maximizing the community welfare (CW):*

$$\left\{\begin{array}{c} \underset{p_t^{\mathrm{S}},p_t^{\mathrm{B}}}{\mathit{Maximize}}\ r(p_t^{\mathrm{S}},p_t^{\mathrm{B}}) \\ \mathit{s.t.}\ \text{(1a)},\ \text{(1b)} \\ \mathit{where}\ e_{itv}^{\mathrm{S}},e_{itv}^{\mathrm{B}} \in \underset{\chi}{\mathit{argmin}}\, C_{iv}(\chi) \\ \mathit{s.t.}\ \text{(1e)–(1l)} \end{array}\right\} \equiv \left\{\begin{array}{c} \underset{p_t^{\mathrm{S}},p_t^{\mathrm{B}}}{\mathit{Maximize}}\ \sum_{itv}\phi_v\Big(\underbrace{r_{itv}(p_t^{\mathrm{S}},p_t^{\mathrm{B}})-C_{iv}(\chi)}_{=CW}\Big) \\ \mathit{s.t.}\ \text{(1a)},\ \text{(1b)} \\ \mathit{where}\ e_{itv}^{\mathrm{S}},e_{itv}^{\mathrm{B}} \in \underset{\chi}{\mathit{argmin}}\, C_{iv}(\chi) \\ \mathit{s.t.}\ \text{(1e)–(1l)} \end{array}\right\} \tag{2}$$

Proof. Proof of this proposition is given in Appendix A.1.

2.3. Proposed stochastic disjunctive program

We solve the bilevel program in (1) by reformulating the problem into a single-level problem. To be able to represent the lower-level problem, which is currently a MILP problem, by the KKT optimality conditions (which are necessary and sufficient), we propose an equivalent relaxed linear programming (LP) formulation of (1). Using Proposition 2, we can omit the binary variables in the constraints (1k) and (1l) in the formulation of the lower-level problem.

Proposition 2. *If we drop the binary variables ψ_{itv} from the MILP model, the optimal solution of the resulting relaxed LP model and its original MILP model are the same.*

[5] Availability of the line capacity ($\overline{W}_t$) can vary due to power-system operation issues such as a line outage at time t.

Proof. We assume that the binary variable ψ_{itv}, (1k), and (1l) do not exist and the BSS unit can charge and discharge simultaneously, i.e., $z_{itv}^{\mathrm{C}} > 0$ and $z_{itv}^{\mathrm{D}} > 0$. Therefore, (1) is an LP problem in this case and the KKT optimality conditions hold. Based on this assumption, the Lagrangian multipliers $\underline{\beta}_{itv}$ and $\underline{\gamma}_{itv}$ are equal to zero. The stationary conditions of the relaxed LP problem are written in (3):

$$p_t^{\mathrm{S}}+\lambda_{itv}^{z}+\overline{\upsilon}_{itv}-\underline{\upsilon}_{itv}=0 : e_{itv}^{\mathrm{S}}, \tag{3a}$$

$$-p_t^{\mathrm{B}}-\lambda_{itv}^{z}+\overline{\mu}_{itv}-\underline{\mu}_{itv}=0 : e_{itv}^{\mathrm{B}}, \tag{3b}$$

$$-\lambda_{itv}^{a}+\Lambda_i\lambda_{i(t+1)v}^{a}-\underline{\tau}_{itv}+\overline{\tau}_{itv}=0 : a_{itv}, \tag{3c}$$

$$\Lambda_i\lambda_{i1v}^{a}-\alpha_{i0v}^{a}=0 : a_{itv}, t=0, \tag{3d}$$

$$P_i^{\mathrm{Q}}-\lambda_{itv}^{a}/\eta_i^{\mathrm{D}}\theta_i^{\mathrm{B}}+\lambda_{itv}^{z}-\underline{\gamma}_{itv}+\overline{\gamma}_{itv}=0 : z_{itv}^{\mathrm{D}}, \tag{3e}$$

$$P_i^{\mathrm{Q}}+\eta_i^{C}\lambda_{itv}^{a}/\theta_i^{\mathrm{B}}-\lambda_{itv}^{z}-\underline{\beta}_{itv}+\overline{\beta}_{itv}=0 : z_{itv}^{\mathrm{C}}. \tag{3f}$$

From (3e) and (3f) we can derive:

$$\lambda_{itv}^{a}/\theta_i^{\mathrm{B}} \overset{(3e)}{=} \eta_i^{\mathrm{D}}(P_i^{\mathrm{Q}}+\lambda_{itv}^{z}-\underline{\gamma}_{itv}+\overline{\gamma}_{itv}) \overset{(3f)}{=} (-P_i^{\mathrm{Q}}+\lambda_{itv}^{z}+\underline{\beta}_{itv}-\overline{\beta}_{itv})/\eta_i^{C}, \tag{4}$$

Based on our assumptions of $z_{itv}^{\mathrm{C}} > 0$ and $z_{itv}^{\mathrm{D}} > 0$, the terms $\underline{\beta}_{itv} = 0$ and $\underline{\gamma}_{itv} = 0$ can be omitted from (4). Therefore,

$$(\frac{1}{\eta_i^{C}}-\eta_i^{\mathrm{D}})\lambda_{itv}^{z}=(\eta_i^{\mathrm{D}}\overline{\gamma}_{itv}+\frac{1}{\eta_i^{C}}\overline{\beta}_{itv})+(\frac{1}{\eta_i^{C}}+\eta_i^{\mathrm{D}})P_i^{\mathrm{Q}}. \tag{5}$$

While the right-hand side of (5) is strictly positive (P_i^{Q}, η_i^{C}, $\eta_i^{\mathrm{D}} > 0$ and $\overline{\beta}_{itv}$, $\overline{\gamma}_{itv} \geq 0$) its left-hand side is negative ($\lambda_{itv}^{z} < 0$ and $\frac{1}{\eta_i^{C}}-\eta_i^{\mathrm{D}} \geq 0$). From this contradiction, one can conclude that the assumption of simultaneous charge and discharge of the BSS ($z_{itv}^{\mathrm{C}} > 0$ and $z_{itv}^{\mathrm{D}} > 0$) cannot hold.[6] □

Thus, the dual feasibility conditions of the LP formulation can be described as:

$$\underline{\beta}_{itv},\overline{\beta}_{itv},\underline{\gamma}_{itv},\overline{\gamma}_{itv},\underline{\mu}_{itv},\overline{\mu}_{itv},\underline{\tau}_{itv},\overline{\tau}_{itv},\underline{\upsilon}_{itv},\overline{\upsilon}_{itv} \geq 0. \tag{6}$$

The complementary slackness conditions for the lower-level problem result in several nonlinear terms but, according to [57], the complementary slackness conditions can be replaced with the strong duality condition. The strong duality condition for the lower-level problem can be formulated as:

$$\begin{aligned} -\sum_t(p_t^{\mathrm{S}}e_{itv}^{\mathrm{S}}-p_t^{\mathrm{B}}e_{itv}^{\mathrm{B}}+P_i^{\mathrm{Q}}(z_{itv}^{\mathrm{C}}+z_{itv}^{\mathrm{D}})) &= -\alpha_{i0v}^{a}\underline{A}_i+ \\ \sum_t(\overline{\tau}_{itv}\overline{A}_i-\underline{\tau}_{itv}\underline{A}_i+\overline{\mu}_{itv}\overline{G}_i+\overline{\upsilon}_{itv}\overline{L}_i-\lambda_{itv}^{z}(G_{itv}-L_{itv}) & \\ +U_{it}\overline{\beta}_{itv}\overline{Z}_i^{\mathrm{C}}+U_{it}\overline{\gamma}_{itv}\overline{Z}_i^{\mathrm{D}}). & \end{aligned} \tag{7}$$

The bilinear terms $p_t^{\mathrm{S}}e_{itv}^{\mathrm{S}}$ and $p_t^{\mathrm{B}}e_{itv}^{\mathrm{B}}$ in the strong duality constraint and the upper-level problem make the reformulated problem a nonlinear programming (NLP) problem. We denote these bilinear terms π_{itv}^{S} and π_{itv}^{B}, respectively. To eliminate the nonlinearity, we introduce discrete electricity sell and buy prices that can take values from a feasible set of prices $p_t^{\mathrm{X}} \in \{P_{1t}^{\mathrm{X}},\ldots,P_{kt}^{\mathrm{X}},\ldots,P_{nt}^{\mathrm{X}}\}$. Accordingly, we formulate the bilinear terms in the following disjunctive form:

$$p_t^{\mathrm{X}}e_{itv}^{\mathrm{X}}=\bigvee_{k=1}^{n}P_{kt}^{\mathrm{X}}e_{itv}^{\mathrm{X}}, \tag{8}$$

where the disjunction is represented by the disjunction (OR) operator $\bigvee$. To shorten the expressions in (8) and throughout this paper, the

[6] Although we have proved Proposition 2 analytically, the proposition statement is also intuitive. It is not economical for a BSS with charging and discharging efficiencies less than 100% to charge and discharge at the same time.

superscript X represents both sell and buy variables and parameters (instead of the superscripts S and B). The original program can therefore be rewritten as a stochastic disjunctive program:

$$\underset{\xi}{\text{Maximize}}\, r = \sum_{v,i,t\neq 0} \phi_v(P^{\mathrm{M}}_{tv}(e^{\mathrm{B}}_{itv}-e^{\mathrm{S}}_{itv})+\bigvee_{k=1}^{N} P^{\mathrm{S}}_{k} e^{\mathrm{S}}_{itv}-\bigvee_{k=1}^{N} P^{\mathrm{B}}_{k} e^{\mathrm{B}}_{itv})$$

Subject to: (1b), (1c), (1e)–(1l), (3), (6),

(7) rewritten with (8). (9)

where ξ is the set of decision variables. $\xi = \{p^{\mathrm{S}}_t, p^{\mathrm{B}}_t, e^{\mathrm{S}}_{itv}, e^{\mathrm{B}}_{itv}, a_{itv}, z^{\mathrm{C}}_{itv}, z^{\mathrm{D}}_{itv}, \lambda^{a}_{itv}, \underline{\tau}_{itv}, \overline{\tau}_{itv}, \underline{\mu}_{itv}, \overline{\mu}_{itv}, \underline{\upsilon}_{itv}, \overline{\upsilon}_{itv}, \underline{\beta}_{itv}, \overline{\beta}_{itv}, \underline{\gamma}_{itv}, \overline{\gamma}_{itv}\}$. Using a binary expansion approach, the disjunctive problem in (9) can be reformulated as a MILP problem. The MILP formulation (presented later in Section 2.5) contains many binary variables, which leads to a high computational effort. Moreover, the performance of the solver depends on the right choice of M^{X}. To improve these shortcomings, authors of [48] suggest an alternative approach to deal with bilinear terms. Similar to [54], we adopt a linear quasi-relaxation to transform this problem to an LP problem and deal with the disjunctive nature of p^{X}_t in our solution algorithm.

To this end, instead of formulating the electricity sell and buy prices as a convex combination of discrete values, we use only their lower and upper bounds. By introducing a continuous variable d^{X}_t, we rewrite p^{X}_t as:

$$p^{\mathrm{X}}_t = \underline{p}^{\mathrm{X}}_t d^{\mathrm{X}}_t + \overline{p}^{\mathrm{X}}_t(1-d^{\mathrm{X}}_t), 0 \le d^{\mathrm{X}}_t \le 1. \tag{10}$$

Therefore, the aggregator's p^{X}_t always adopts a value between $\underline{p}^{\mathrm{X}}_t$ and $\overline{p}^{\mathrm{X}}_t$. Then, the disjunctive constraints can be enforced by:

$$\bigvee_{k=1}^{N}\left[\underline{p}^{\mathrm{X}}_t d^{\mathrm{X}}_t + \overline{p}^{\mathrm{X}}_t(1-d^{\mathrm{X}}_t) = P^{\mathrm{X}}_{kt}\right]. \tag{11}$$

To perform the quasi-relaxation method, we rewrite e^{X}_{itv}, which appears in the bilinear term π^{X}_{itv}, as the summation of two non-negative variables:

$$e^{\mathrm{X}}_{itv} = e^{\mathrm{X}(0)}_{itv} + e^{\mathrm{X}(1)}_{itv}. \tag{12}$$

Therefore, the bilinear term π^{X}_{itv} can be formulated as:

$$\pi^{\mathrm{X}}_{itv} = (e^{\mathrm{X}(0)}_{itv} + e^{\mathrm{X}(1)}_{itv})\left[\underline{p}^{\mathrm{X}}_t d^{\mathrm{X}}_t + \overline{p}^{\mathrm{X}}_t(1-d^{\mathrm{X}}_t)\right]. \tag{13}$$

We solve the formulated disjunctive program using an MBB algorithm, which branches on the ranges of sell and buy prices instead of branching on binary variables. To obtain the upper bound of the objective value, we apply quasi-relaxation of the problem and drop the disjunctive constraint (11) and replace (13) with (14):

$$\pi^{\mathrm{X}}_{itv} = e^{\mathrm{X}(0)}_{itv}\underline{p}^{\mathrm{X}}_t + e^{\mathrm{X}(1)}_{itv}\overline{p}^{\mathrm{X}}_t, \tag{14a}$$

$$0 \le e^{\mathrm{X}(0)}_{itv} \le M^{\mathrm{X}} d^{\mathrm{X}}_t, \tag{14b}$$

$$0 \le e^{\mathrm{X}(1)}_{itv} \le M^{\mathrm{X}}(1-d^{\mathrm{X}}_t), \tag{14c}$$

$$0 \le d^{\mathrm{X}}_t \le 1. \tag{14d}$$

As a result, the disjunctive program (9) can be reformulated in the following quasi-relaxed form:

SDPQ: $\underset{\varrho}{\text{Maximize}}\, r = \sum_{v,i,t} \phi_v(P^{\mathrm{M}}_{tv}(e^{\mathrm{B}}_{itv}-e^{\mathrm{S}}_{itv})+\pi^{\mathrm{S}}_{itv}-\pi^{\mathrm{B}}_{itv})$

subject to: (1b), (1c), (1e)–(1l), (3), (6),

(7) rewritten with π^{X}_{itv} from (14), (12). (15)

where $\varrho = \{p^{\mathrm{S}}_t, p^{\mathrm{B}}_t, e^{\mathrm{S}}_{itv}, e^{\mathrm{S}(0)}_{itv}, e^{\mathrm{S}(1)}_{itv}, e^{\mathrm{B}}_{itv}, e^{\mathrm{B}(0)}_{itv}, e^{\mathrm{B}(1)}_{itv}, a_{it}, z^{\mathrm{C}}_{itv}, z^{\mathrm{D}}_{itv}, d^{\mathrm{S}}_t, d^{\mathrm{B}}_t, \lambda^{a}_{itv}, \underline{\tau}_{itv}, \overline{\tau}_{itv}, \underline{\mu}_{itv}, \overline{\mu}_{itv}, \underline{\upsilon}_{itv}, \overline{\upsilon}_{itv}, \underline{\beta}_{itv}, \overline{\beta}_{itv}, \underline{\gamma}_{itv}, \overline{\gamma}_{itv}\}$ is the set of decision variables. For simplicity, we will refer to the quasi-relaxed formulation of the stochastic disjunctive program in (15) as SDPQ.

2.4. MBB solution algorithm

We now explain the different steps of the MBB algorithm in solving the SDPQ. Having imposed the dropped constraint in the quasi-relaxation, we partition the disjunctive steps dynamically to find the solution of (1) efficiently. The dynamic partitioning feature addresses the limitation of the disjunctive formulation in having a fixed number of discrete steps.

Fig. 3 illustrates the different steps of the algorithm in detail.

Initialization: The algorithm starts by initializing the parameters $\underline{p}^{\mathrm{X}}_t$, $\overline{p}^{\mathrm{X}}_t$, $\underline{H}^{\mathrm{X}}_t$, and $\underline{H}^{\mathrm{X}}_t$ as well as the algorithm hyperparameters LB and S^{X}:

$$\underline{p}^{\mathrm{X}}_t \leftarrow P^{\mathrm{X}}_{1t},\ \overline{p}^{\mathrm{X}}_t \leftarrow P^{\mathrm{X}}_{nt}, \tag{16a}$$

$$\underline{H}^{\mathrm{X}}_t \leftarrow \underline{P}^{\mathrm{X}},\ \overline{H}^{\mathrm{X}}_t \leftarrow \overline{P}^{\mathrm{X}}, \tag{16b}$$

$$\mathrm{LB} \leftarrow -\infty,\ S^{\mathrm{X}} \leftarrow (\overline{P}^{\mathrm{X}} - \underline{P}^{\mathrm{X}})/(|k|-1), \tag{16c}$$

$$P^{\mathrm{X}}_{kt} = \underline{H}^{\mathrm{X}}_t + k(\overline{H}^{\mathrm{X}}_t - \underline{H}^{\mathrm{X}}_t)/|k|. \tag{16d}$$

where $\underline{H}^{\mathrm{X}}_t$ and $\overline{H}^{\mathrm{X}}_t$ are intermediary lower and upper levels of disjunctive values in each time step, and S^{X} is the disjunction step size and LB is the lower bound of the solution that represents the best solution so far. In (16d), the disjunctive values P^{X}_{kt} for each time step are calculated.

Solving SDPQ and generating new branches: In each iteration (itr in short), the algorithm solves the quasi-relaxed formulation of the problem (SDPQ) in (15). If the problem is infeasible or the upper bound of the objective function (r) is less than LB, the nodes are fathomed. For the cases with r higher than LB ($r \ge$ LB), the algorithm checks the condition (17) to make sure that the result of the SDPQ is identical to (1) and the relaxed constraint in (11) is imposed.

$$d^{\mathrm{X}}_t \in \{0,1\} \vee \underline{p}^{\mathrm{X}}_t = \overline{p}^{\mathrm{X}}_t. \tag{17}$$

If condition (17) is valid for all the optimization time steps, the node is fathomed, LB is updated ($LB \leftarrow r$), and the values of $\underline{p}^{\mathrm{X}}_t$ and $\overline{p}^{\mathrm{X}}_t$ are stored in intermediary parameters $\underline{p}^{\mathrm{X}\star}_t$ and $\overline{p}^{\mathrm{X}\star}_t$. The results with $d^{\mathrm{X}}_t \notin \{0,1\}$, $\underline{p}^{\mathrm{X}}_t \neq \overline{p}^{\mathrm{X}}_t$ indicate that p^{X}_t is not discrete (i.e., $p^{\mathrm{X}}_t \notin \{P^{\mathrm{X}}_{1t}, \dots, P^{\mathrm{X}}_{kt}, \dots, P^{\mathrm{X}}_{nt}\}$) and therefore does not satisfy constraint (11). In these cases, we keep the nodes active and **generate new branches**. According to (18a), the algorithm finds the closest disjunctive value and generates two new branches on either side of the p^{X}_t (18b):

$$P^{\mathrm{X}}_{kt} \le \underline{p}^{\mathrm{X}}_t d^{\mathrm{X}}_t + \overline{p}^{\mathrm{X}}_t(1-d^{\mathrm{X}}_t), \tag{18a}$$

$$\overline{p}^{\mathrm{X}}_t = P^{\mathrm{X}}_{kt} \text{ and } \underline{p}^{\mathrm{X}}_t = P^{\mathrm{X}}_{(k+1)t}. \tag{18b}$$

After creating new branches, the algorithm evaluates all the nodes and selects the one with the largest LB as the next node to assess. We chose this branching method as it creates fewer sub-problems and, therefore, reduces the computational time required [58]. The next node is evaluated by repeating this step.

Dynamic partitioning: Each optimization "round" is terminated when all the created nodes have been investigated. Once there are no branches left to solve, if LB is equal to its initial value (i.e., $-\infty$), the problem is infeasible. If not (i.e., the algorithm has found at least one solution to the problem), we discretize the solution range further to search for values that may lie between the first disjunctive steps and we start a new round of optimization. Changes in the solution range ($\underline{p}^{\mathrm{X}}_t$ to $\overline{p}^{\mathrm{X}}_t$) are schematically visualized in Fig. 4. To perform the dynamic partitioning, we update $\overline{H}^{\mathrm{X}}_t$ and $\underline{H}^{\mathrm{X}}_t$ with the lower and upper values of the best solution:

$$\overline{H}^{\mathrm{X}}_t \leftarrow \overline{p}^{\mathrm{X}\star}_t, \underline{H}^{\mathrm{X}}_t \leftarrow \underline{p}^{\mathrm{X}\star}_t \tag{19}$$

If $\underline{p}^{\mathrm{X}}_t$ and $\overline{p}^{\mathrm{X}}_t$ have adopted the same value ($\underline{p}^{\mathrm{X}}_t = \overline{p}^{\mathrm{X}}_t$), at least one of them is moved by the size of one step S^{X}:

$$\text{If } \underline{p}^{\mathrm{X}}_t = \overline{p}^{\mathrm{X}}_t = \underline{P}^{\mathrm{X}} \text{ then } \overline{H}^{\mathrm{X}}_t \leftarrow \underline{p}^{\mathrm{X}}_t + S^{\mathrm{X}}, \tag{20a}$$

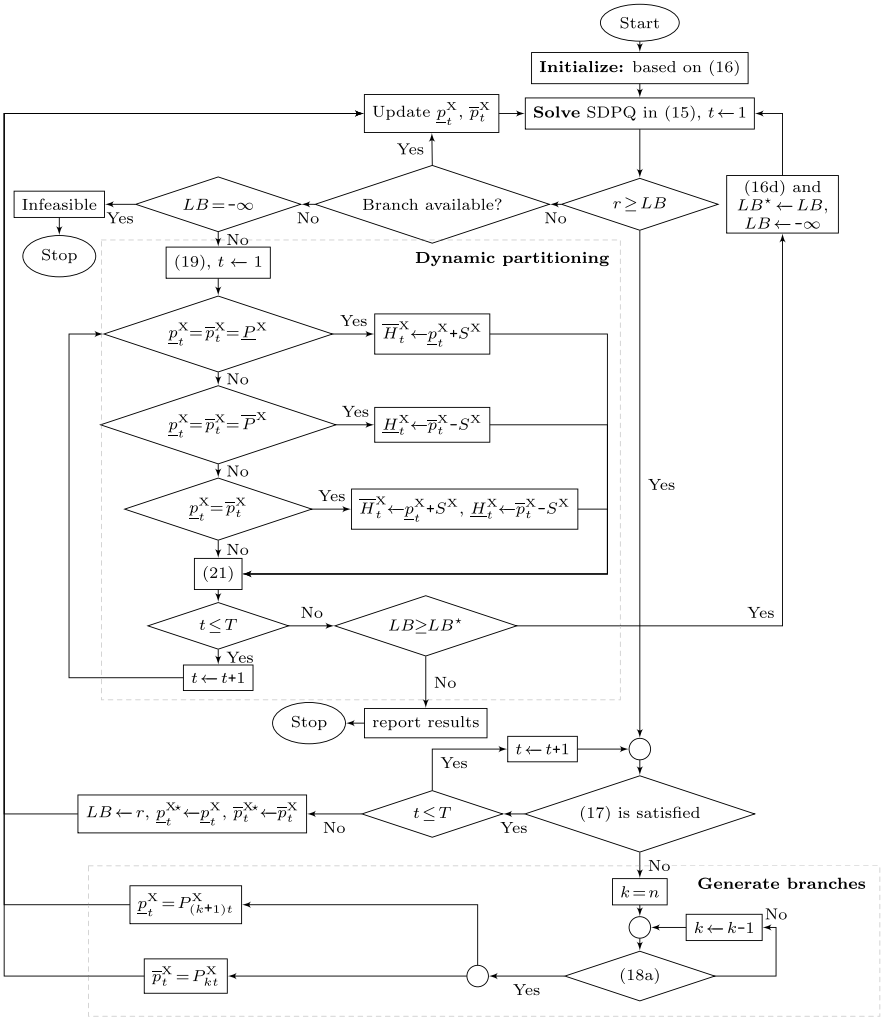

Fig. 3. Our proposed modified branch-and-bound (MBB) algorithm.

Else if $\underline{p}_t^X = \overline{p}_t^X = \overline{P}^X$ then $\underline{H}_t^X \leftarrow \overline{p}_t^X - S^X$, (20b)

Else $\{\overline{H}_t^X \leftarrow \underline{p}_t^X + S^X$ and $\underline{H}_t^X \leftarrow \overline{p}_t^X - S^X\}$ (20c)

Finally, we update the values of $\underline{p}_t^X$ and $\overline{p}_t^X$ once more, set the LB to $-\infty$, update the disjunctive values according to (16d), and solve the problem again.

$$\overline{p}_t^X \leftarrow \overline{H}_t^X, \underline{p}_t^X \leftarrow \underline{H}_t^X \tag{21}$$

If the solution (LB) is improved, the algorithm continues. Otherwise, the optimal solution is reported.

2.5. Benchmark models

To assess the performance of the proposed MBB algorithm, we solve the bilevel program with two alternative algorithms, as described in Sections 2.5.1 and 2.5.2.

2.5.1. MILP

To reformulate the disjunctive problem in (9) as a MILP problem, we use a binary expansion approach. For the disjunctive term $\bigvee_{k=1}^{n} P_{kt}^X e_{itv}^X$, we introduce binary variables $\sum_{k=1}^{N} b_{tvk}^X = 1$ and rewrite the disjunctive constraints as:

$$-M^X b_{tvk}^X \leq h_{itkv}^X \leq M^X b_{tvk}^X, \forall itvk, \tag{22a}$$

$$-M^X(1 - b_{tvk}^X) \leq h_{itkv}^X - P_{kt}^X e_{itv}^S \leq M^X(1 - b_{tvk}^X), \forall itvk, \tag{22b}$$

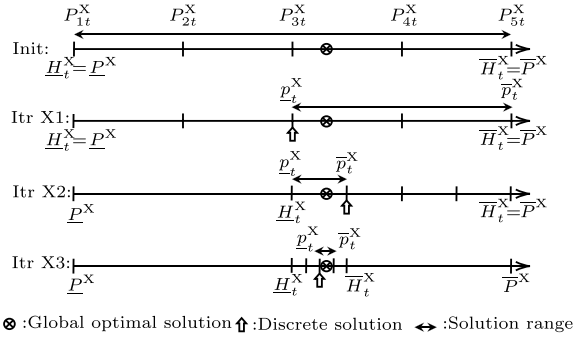

Fig. 4. Change of the solution range ($\overline{p}_t^X$ to $\underline{p}_t^X$) in our proposed MBB algorithm. Itr X1, X2 and X3 respectively refer to the iterations with the best solutions in the first, second, and third rounds of optimization.

where M^X is a sufficiently large number, and h_{itkv}^X are continuous variables that are enforced to take the values of the binary terms for a single step k. The disjunctive term and the prices can then be written as:

$$\bigvee_{k=1}^{N} P_{kt}^X e_{itv}^X = \sum_{k=1}^{N} h_{itkv}^X, \tag{23a}$$

$$p_t^{\mathrm{X}} = \sum_{k=1}^{N} P_{kt}^{\mathrm{X}} b_{tvk}^{\mathrm{X}}. \tag{23b}$$

The disjunctive problem in (9) together with additional constraints derived in (22) and (23) can be solved using standard commercial MILP solvers and branch-and-bound algorithms.

2.5.2. Special branch-and-bound (SBB) algorithm

To demonstrate the improvements resulting from the MBB algorithm, we also solve SDPQ using the SBB algorithm proposed in [54].

2.6. Benchmark tariffs

As shown in Proposition 1, we expect that the competition between the aggregator and users in the proposed ORTP strategy increases the CW of the EC, defined as $\mathrm{CW} = r - C'$, where $C' = \sum_{itv} \phi_v C_{iv}$ is the total cost of users. Note that, in the calculation of CW, the terms with p_t^{X} are eliminated. Therefore, $\mathrm{CW} = \sum_{itv} \phi_v P_{tv}^{\mathrm{M}} (e_{itv}^{\mathrm{S}} - e_{itv}^{\mathrm{B}}) + P_i^{\mathrm{Q}} (z_{itv}^{\mathrm{C}} + z_{itv}^{\mathrm{D}})$. To validate our hypothesis regarding the impact of competition on the CW, we compare the resulting CW values from the ORTP with those gained from the two benchmarks.

- *Average pricing* (AP) uses the mean value of the market prices during the simulated period to calculate p_t^{X}. Therefore, the tariff does not contain any real-time element and the price is constant over time, similar to the retail price in many countries:

$$p_t^{\mathrm{X}} = \Big(\sum_{t}^{\overline{T}} P_{tv}^{\mathrm{M}}\Big)/|t| + \Gamma^{\mathrm{X}}. \tag{24}$$

- *Real-time pricing* (RTP) includes the market price signals in p_t^{X}:

$$p_t^{\mathrm{X}} = P_{tv}^{\mathrm{M}} + \Gamma^{\mathrm{X}}. \tag{25}$$

While the aggregator's margin in the ORTP is optimized and may change in real time, the parameters Γ^{X} in Eqs. (24) and (25) are exogenous model assumptions that do not vary over time. We assume that $\Gamma^{\mathrm{S}} = -\Gamma^{\mathrm{B}}$, and this is set at 0.5 ¢/kWh. Since, in the calculation of CW, the terms with p_t^{X} are eliminated, the choice of Γ^{X} does not have any impact on the community's welfare.

2.7. Data and model parameterization

For the household demand profiles, we use the data from [59]. This dataset contains high-resolution measured load profiles of 74 different German households. Data regarding the load and availability profiles of EVs were obtained using the open-source tool VencoPy [60], based on the mobility data available in [61]. The translation of the mobility data into the EV electrical demand and charging availability profiles for this analysis is described in Appendix A.2. The electricity generation profile of the PV systems is scaled based on the share of generated electricity from the installed PV capacity in 2018 in Germany (PV capacity data was collected from [62]). For P_{tv}^{M}, we use the day-ahead electricity market prices for Germany in [62]. The aggregator's maximum (minimum) sell price $\overline{P}^{\mathrm{S}}$ ($\underline{P}^{\mathrm{S}}$) is 8 (3) ¢/kWh, while the maximum (minimum) buy price $\overline{P}^{\mathrm{B}}$ ($\underline{P}^{\mathrm{B}}$) is 7 (2) ¢/kWh. The marginal cost of charging and discharging the battery (P_i^{Q}) is 1 ¢/kWh. The SOC of the BSSs cannot drop below 0 or exceed a maximum value of 1 ($0 \le \overline{A}_i \le 1$). For the user-specific model parameters (Y), we assume the values listed in Table 3. The big-M parameters (M^{S} and M^{B}) in the MILP and LP formulations are set to 100000. Other parameters will be introduced for each case study in the next section.

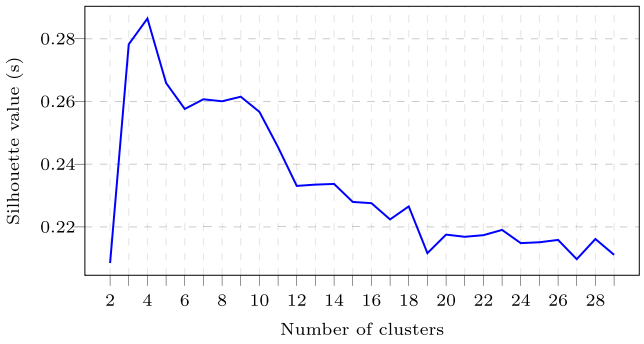

Fig. 5. Silhouette values for different numbers of clusters.

2.8. MPCB scenario generation

The uncertain *attributes* in SDPQ are the market price, demand and PV generation of each user. Since these attributes vary continuously over time and with temperature, wind speed, cloud cover, etc., the aggregator needs to take their associated uncertainties into account. One approach to generating the required scenarios for the optimization is the so-called direct-sampling method, which samples directly from the historical data. Using this approach, if we increase the size of the sample, the distribution of the scenarios will converge to the actual distribution of the data. However, performing the optimization for many scenarios requires excessive computational resources and is impractical. To provide a **practical** number of scenarios that are **representative** of the historical data, we propose the following MPCB scenario-generation algorithm:

Step 1: The time series for all attributes is specified according to year, month, week, day of the week and hour of the day. Then, the data for all attributes are scaled to the range [−1,1] so that we can use the Euclidean distance to compare similarities between different data points. The vector of attributes $\mathbf{x}$ has a probability distribution function $f(\mathbf{x})$.

Step 2: The data for the attributes are divided into $|\{C\}|$[7] clusters. We employ the well-known k-means method to group the $\dim(\mathbf{x})$ data into clusters. To decide on the suitable number of clusters, we perform a sensitivity analysis by applying the k-means method for different numbers of clusters and choose a value of $|C|$ that demonstrates the highest silhouette value. The silhouette value $s(\mathbf{p})$ is calculated in (26), in which $d(\mathbf{p})$ is the average Euclidean distance between point $\mathbf{p}$ and all the points in its cluster. In this equation, $d'(\mathbf{p})$ is the smallest average Euclidean distance between point $\mathbf{p}$ and all the points in other clusters [63]. A larger average silhouette value, i.e., $\sum_{\mathbf{p}} s(\mathbf{p})/\dim(\mathbf{x})$, indicates better cohesion within and separation between the clusters.

$$s(\mathbf{p}) = \begin{cases} 1 - d(\mathbf{p})/d'(\mathbf{p}), & \text{if } d(\mathbf{p}) < d'(\mathbf{p}) \\ 0, & \text{if } d(\mathbf{p}) = d'(\mathbf{p}) \\ d'(\mathbf{p})/d(\mathbf{p}) - 1, & \text{if } d(\mathbf{p}) > d'(\mathbf{p}) \end{cases} \tag{26a}$$

$$-1 \le s(\mathbf{p}) \le 1 \tag{26b}$$

The average silhouette values for different numbers of clusters are plotted in Fig. 5. We select $|\{C\}| = 4$, which results in the highest silhouette value, as the optimal number of clusters for the k-means clustering. Moreover, we only retain the attributes that improve the silhouette value. These attributes are the hour of day, day of the week, market prices, load, and solar generation profiles.

[7] The expression $|\{Q\}|$ is used for cardinality of the set $\{Q\}$.

Table 3
Users' technical parameters.

Y [−]	θ_i^{B} [kWh]	η_i^{C} [−]	η_i^{D} [−]	Λ_i [−]	$\overline{Z}_i^{\mathrm{C}}$ [kW]	$\overline{Z}_i^{\mathrm{D}}$ [kW]	$\overline{G}_i$ [kW]	$\overline{L}_i$ [kW]	P_i^{Q} [¢/kWh]	θ_i^{PV} [kW]	BSS [−]
1	20	1	1	1	20	20	20	20	1	20	HES
2	0.01[a]	0	0.01[a]	0	0	0	20	20	0	0	✗
3	10	0.95	0.95	0.99	10	10	20	20	1	10	HES
4	6	0.90	0.90	1	6	6	20	20	1	7	HES
5	50	0.98	0.98	1	50	50	11	11	1	0	EV

[a]User 2 does not own a BSS. To avoid division by zero, a very small number is chosen for its θ_i^{B} and η_i^{D}.

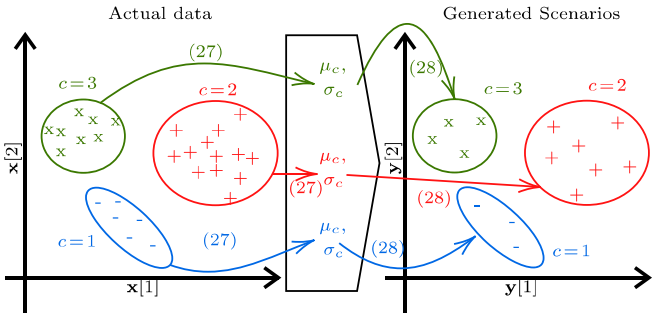

Fig. 6. Illustrative representation of the scenario-generation algorithm.

Step 3: The mean (μ_c) and standard deviation (σ_c) of the data in each cluster $c \in C$ are calculated as:

$$\mu_c = E(\mathbf{x}) = \int \mathbf{x} f(\mathbf{x}) \mathrm{d}x \tag{27a}$$

$$\sigma_c = \sqrt{E((\mathbf{x}-\mu_c)^2)} = \sqrt{\int (\mathbf{x}-\mu_c)^2 f(\mathbf{x}) \mathrm{d}x}. \tag{27b}$$

We then use these values are to generate scenarios in each cluster separately. Using the calculated means and standard deviations for each cluster, we generate a vector of random numbers $\mathbf{y}$ with a normal distribution:

$$\mathbf{y} = [\mathbf{y}_c] \text{ and } g(\mathbf{y}_c) \equiv N(\mu_c, \sigma_c). \tag{28}$$

Here, $N(\mu_c, \sigma_c)$ is a normal distribution function with a mean value of μ_c and a standard deviation of σ_c. The data within each cluster show significantly higher cohesion compared to the alternative of not using these clusters, e.g., direct sampling. Fig. 6 shows a simplified representation of the scenario-generation algorithm for three clusters ($|\{C\}| = 3$) in two dimensions. Note that, depending on the number of attributes, the actual number of dimensions dim($\mathbf{x}$) could be greater than 2.

Fig. 7 shows a comparison of the means and standard deviations of the actual data (described in Section 2.7) with the scenarios generated by the direct-sampling and the MPCB approaches. It can be seen that the distribution of the generated scenarios using the MPCB algorithm for all attributes are closer to the actual data when compared to the direct-sampling approach.

3. Case studies

In this section, we consider four case studies to demonstrate the performance of the methodology. The first three are illustrative examples to show how the algorithm and pricing work. The fourth is a larger-scale example to demonstrate computational scalability. Table 4 gives an overview of the model setups of the different case studies.

Table 4
Overview of model setups in the case studies.

Case study	$\overline{T}$	i	v	Y	Demonstration goal
I	2	1	1	1	Convergence of the solution algorithm
II	4	1	1	1	Determination of ORTP
III	4	2	1	1,2	Internal balance of load and generation
IV	8	5	9	1,2,3,4,5	Large-scale stochastic optimization

3.1. Case study I

In the first example, we consider a single prosumager ($i = 1$), parameterized with $Y = 1$, an optimization period of 2 h ($t \in \{1,2\}$), one scenario with probability of 1 ($|\{v\}| = 1$, $\phi_v = 1$), and three discretization steps ($k = 3$). The prosumager has a constant demand of 5 kWh ($L_{itv}|_{(t=1)} = L_{itv}|_{(t=2)} = 5$ kWh), and the power generation is 7 kWh and 3 kWh in the first and second time steps, respectively ($G_{itv}|_{(t=1)} = 7$ kWh, $G_{itv}|_{(t=2)} = 3$ kWh). The market price changes from 0 ¢/kWh in $t = 1$ to 8 ¢/kWh in $t = 2$ ($P_{tv}^{\mathrm{M}}|_{t=1} = 0$ ¢/kWh, $P_{tv}^{\mathrm{M}}|_{t=2} = 8$ ¢/kWh). The BSS is available all the time ($U_{it} = 1$). The discrete options for sell and buy prices are $p_t^{\mathrm{S}} \in \{3, 5.5, 8\}$ and $p_t^{\mathrm{B}} \in \{2, 4.5, 7\}$, respectively. Detailed results for the performance of the proposed solution algorithm are shown in Table 5.

The proposed MBB algorithm changes $\underline{p}_t^{\mathrm{S}}$, $\overline{p}_t^{\mathrm{S}}$, $\underline{p}_t^{\mathrm{B}}$, and $\overline{p}_t^{\mathrm{B}}$ at each iteration. In iterations 1 to 7, condition (17) is not satisfied (status A). Iteration 8 is the first iteration in which all solutions are discrete for all time periods (status B: condition (17) is fulfilled). Since $r \geq$ LB and all the solutions are discrete, LB is updated for the first time from −1000 to −14 in iteration 9. Similarly, $\underline{p}_t^{\mathrm{X}}$ and $\overline{p}_t^{\mathrm{X}}$ are changed until better solutions are found in iterations 25, 48, and 53 and the lower bound updates to 72 (LB=72). After 56 iterations, the algorithm has checked all the branches and this round is ended (status C). Therefore, the highest profit for the aggregator with the current discretization steps is 72 ($r = 72$ ¢). Thus, if we use the SBB algorithm proposed in [54] with fixed discrete steps, the optimal solution will be 72 in iteration 53, and the algorithm will stop after iteration 56. In contrast, in the proposed MBB algorithm, we modify the discrete steps inside the algorithm to find a solution that is closer to the global optimal point. In iteration 57, we apply the dynamic partitioning technique and start a new round in our algorithm (status D). Based on the best discrete result of the last round, the new discrete options for sale and purchase prices in the new round are $p_1^{\mathrm{B}} \in \{2, 3.25, 4.5\}$, $p_2^{\mathrm{B}} \in \{4.5, 5.75, 7\}$, $p_1^{\mathrm{S}} \in \{3, 4.25, 5.5\}$, and $p_2^{\mathrm{S}} \in \{5.5, 6.75, 8\}$.

As the choices are changed, the LB is initialized again with −1000. Then, $\underline{p}_t^{\mathrm{X}}$ and $\overline{p}_t^{\mathrm{X}}$ are changed until a better discrete solution is found at iterations 71, 83, and 84 with the aggregator's profit r and LB equal to 0, 94, and 94.5. Round 2 of the algorithm is finished after iteration 92. After this, the discrete options are updated once more: $p_1^{\mathrm{B}} \in \{2, 3.25, 4.5\}$, $p_2^{\mathrm{B}} \in \{5.75, 6.375, 7\}$, $p_1^{\mathrm{S}} \in \{3, 4.25, 5.5\}$ and $p_2^{\mathrm{S}} \in \{6.75, 7.375, 8\}$. In round 3, the lower bound of the problem updates twice, in iteration 99 and 101, to 0 and 105.75, respectively. Fig. 8 shows the transformation of the solution range for the purchase price (p_t^{B}) in the time step $t = 2$ in iterations 53, 84, and 101. The remaining

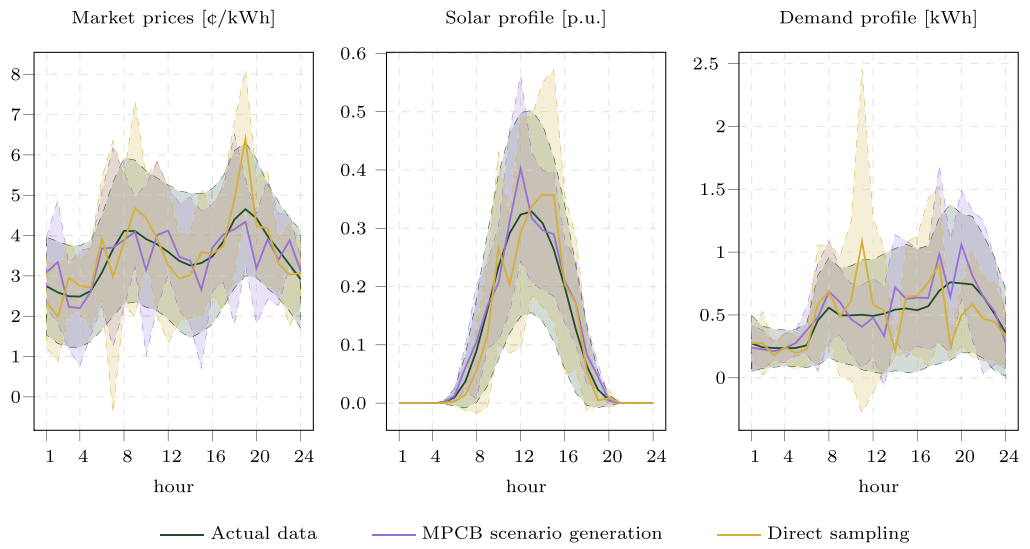

Fig. 7. Comparison of means and standard deviations between MPCB scenario generation, direct sampling, and actual data (sources: [59,62]). Mean values are illustrated with continuous lines. Standard deviations are shown with dashed lines as confidence intervals.

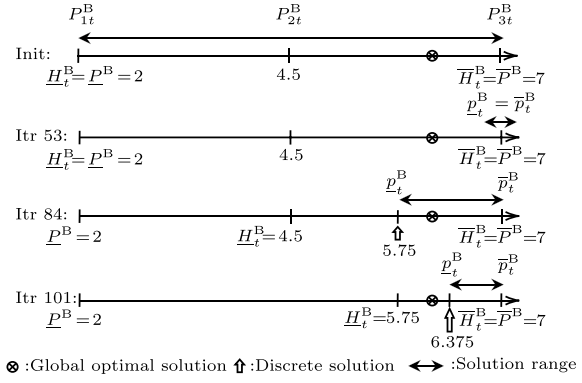

Fig. 8. Change of solution range ($\overline{p}_t^{\mathrm{B}}$ to $\underline{p}_t^{\mathrm{B}}$) in Case I for $t = 2$.

options for $\underline{p}_t^{\mathrm{X}}$ and $\overline{p}_t^{\mathrm{X}}$ are investigated until iteration 104, after which the MBB algorithm for this problem is ended. To reach this objective value with the SBB algorithm, a larger number of discretization steps (k) and correspondingly more iterations are required.

3.2. Case study II

In the second example, the bilevel problem for a simple setup with one prosumager ($i = 1$), parameterized with $Y = 1$, is solved. For a time period of 4 h ($\overline{T} = 4$) and a single scenario, the model results, electricity prices, and prosumager's grid interactions, as well as the input time series, P^{M}, $G_{itv}|_{(Y=1)}$, and $L_{itv}|_{(Y=1)}$, are shown in Fig. 9.

In time steps $t = 3$ and 4, the prosumager uses its generation to cover its load. Note that in our model, the self-consumption of electricity by prosumagers is considered to be free of charge. Therefore, it is profitable for the users to use the generated electricity mainly to cover the own load in most cases. Since the storage is full in this hour, the residual generation at $t = 4$ is fed into the grid. As the highest market price occurs at $t = 4$ ($P_{tv}^{\mathrm{M}}|_{(t=4)} = 9$ ¢/kWh), the aggregator increases the purchase price to $p_t^{\mathrm{B}}|_{(t=4)} = 5.75$ ¢/kWh and incentivizes the prosumager to discharge the storage. The prosumager completely

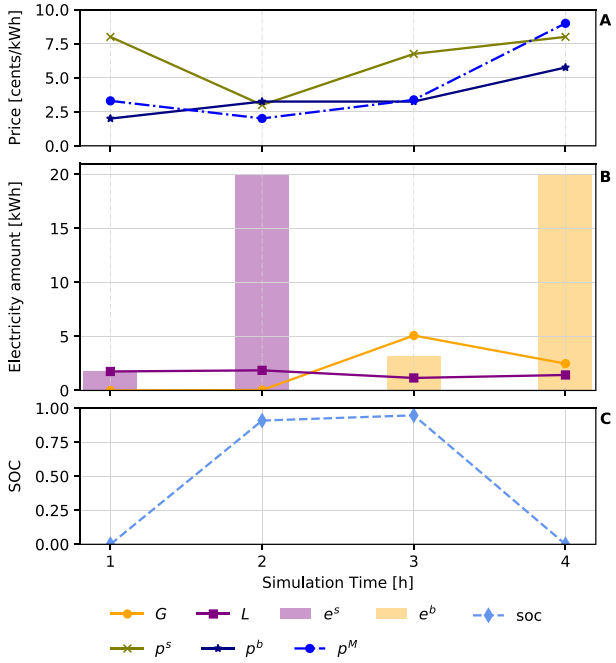

Fig. 9. Optimization results for Case study II. A: Aggregator's and market prices. B: Prosumager's electricity demand and generation, as well as grid usage and feed-in. C: Battery SOC of the prosumager.

discharges the BSS in this time step and feeds 20 kWh into the grid ($e_{itv}^{\mathrm{B}}|_{(t=4)} = \overline{G}_i = 20$ kWh).

3.3. Case study III

In Case study III, we demonstrate how the ORTP reacts to market prices, limited available line capacity, and the availability of local generation and storage. Two users with the technical specifications of $Y = 1$ and 2 (see Table 3) are considered. User 2 ($Y = 2$) does not have a PV system or BSS. Therefore, this user does not have electricity generation and cannot have a flexible interaction with the

Table 5
Detailed results of Case I.

Iteration [−]	t [h]	r [¢]	LB [¢]	p_t^S *	p_t^B *	$\underline{p}_t^S$ *	$\overline{p}_t^S$ *	$\underline{p}_t^B$ *	$\overline{p}_t^B$ *	Round [-]	Status
1	1 2	108	−1000	3 4	2 2.0005	3 3	8 8	2 2	7 7	1	A
2	1 2	106	−1000	3 3	2 2.0006	3 3	8 3	2 2	7 7	1	A
3	1 2	108	−1000	6 8	6 2.0005	3 5.5	8 8	2 2	7 7	1	A
⋮	⋮	⋮	⋮	⋮	⋮	⋮	⋮	⋮	⋮	⋮	⋮
8	**1** **2**	**−14**	**−1000**	**8** **3**	**2** **2**	**3** **3**	**8** **3**	**2** **2**	**2** **2**	**1**	**B**
9	1 2	55.6	−14	7.9990 3	4.5002 2	3 3	8 3	4.5 2	7 2	1	A
⋮	⋮	⋮	⋮	⋮	⋮	⋮	⋮	⋮	⋮	⋮	⋮
53	**1** **2**	**72**	**69**	**3** **8**	**2** **7**	**3** **8**	**3** **8**	**2** **7**	**2** **7**	**1**	**B**
⋮	⋮	⋮	⋮	⋮	⋮	⋮	⋮	⋮	⋮	⋮	⋮
56	1 2	−14	72	5.5 5.5	4.5 4.5	5.5 5.5	5.5 5.5	4.5 2	4.5 4.5	1	C
57	1 2	108	−1000	5.4995 6.9996	4.5 6.9996	3 5.5	5.5 8	2 4.5	4.5 7	2	D
⋮	⋮	⋮	⋮	⋮	⋮	⋮	⋮	⋮	⋮	⋮	⋮
71	**1** **2**	**0**	**−1000**	**3** **5.5**	**2** **4.5**	**3** **5.5**	**3** **8**	**2** **4.5**	**2** **4.5**	**2**	**B**
⋮	⋮	⋮	⋮	⋮	⋮	⋮	⋮	⋮	⋮	⋮	⋮
83	**1** **2**	**94**	**0**	**3** **5.5**	**2** **5.75**	**3** **5.5**	**3** **5.5**	**2** **5.75**	**2** **7**	**2**	**B**
84	**1** **2**	**94.5**	**94**	**3** **6.75**	**2** **5.75**	**3** **6.75**	**3** **8**	**2** **5.75**	**2** **7**	**2**	**B**
⋮	⋮	⋮	⋮	⋮	⋮	⋮	⋮	⋮	⋮	⋮	⋮
92	1 2	0	94.5	5.5 6.75	4.5 5.75	5.5 6.75	5.5 6.75	3.25 4.5	4.5 5.75	2	C
93	1 2	108	−1000	5.4999 8	4.5 7	3 6.75	5.5 8	2 5.75	4.5 7	3	D
⋮	⋮	⋮	⋮	⋮	⋮	⋮	⋮	⋮	⋮	⋮	⋮
99	**1** **2**	**0**	**−1000**	**5.5** **8**	**4.5** **7**	**5.5** **8**	**5.5** **8**	**2** **5.75**	**4.5** **7**	**3**	**B**
⋮	⋮	⋮	⋮	⋮	⋮	⋮	⋮	⋮	⋮	⋮	⋮
101	**1** **2**	**105.75**	**0**	**4.25** **6.75**	**2** **6.375**	**3** **6.75**	**4.25** **8**	**2** **6.375**	**3.25** **7**	**3**	**B**
⋮	⋮	⋮	⋮	⋮	⋮	⋮	⋮	⋮	⋮	⋮	⋮
104	1 2	94.5	105.75	3 8	3 5.75	3 6.75	3 8	2 5.75	3.25 5.75	3	C

*: [¢/kWh]. A: (17) is not fulfilled. B: (17) is fulfilled. LB will be updated. C: All branches are checked. End of this round. D: Dynamic partitioning is applied. Beginning of a new round. Highlighted solution: Best solution in this round.

grid. Moreover, we assume that the available line capacity is limited ($\overline{W}|_{(t=1,2,4)} = 20$ kWh and $\overline{W}|_{(t=3)} = 0.6$ kWh). The optimization results and the input series for Case III are presented in Fig. 10. As a result of a low market price at $t = 2$, the aggregator offers a low sale price to the users. However, due to the restricted available line capacity, user 1 cannot charge the BSS completely ($e^S_{itv}|_{(t=2)} = 17.526$ kWh, $a_{itv}|_{(t=2)} = 0.78$). In hour 3 ($t = 3$), user 1 feeds enough electricity into the community grid to cover the load of user 2 and therefore the load and generation of the EC can be balanced locally in this hour. At $t = 4$, the market price reaches its highest value ($P^M_{tv}|_{(t=4)} = 8.9$). Therefore, the aggregator increases the purchase price to $p^B_t|_{(t=5)} = 5$ ¢/kWh and user 1 is encouraged to discharge its battery completely.

3.4. Case study IV

In Case study IV, we increase the problem size and analyze an EC with a larger number of users and a longer optimization period compared to the previous illustrative examples. Five users ($|\{i\}| = 5$) and eight optimization periods (i.e., $|\{t\}| = 8$) are considered. These users are relatively diverse and adopt the parameters shown

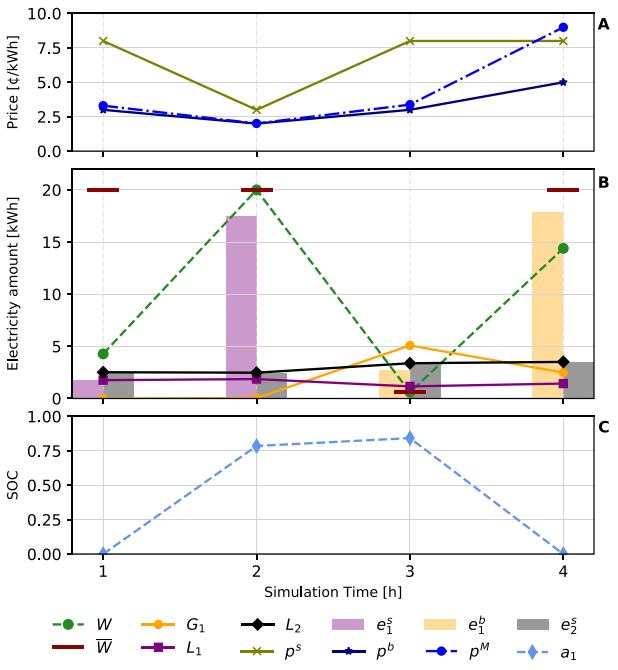

Fig. 10. Optimization results for Case study III. A: Aggregator's and market prices. B: Users' electricity demand and generation, as well as grid usage and feed-in. C: Battery SOC of the prosumager.

in Table 3. For this case, we study the sensitivity of the aggregator's expected profit to the scenarios. In a simulation experiment, we vary the number of scenarios ($|\{v\}|$) from 1 (indicating a deterministic solution) to 50 and solve the SDPQ over 7000 times.[8] We use the MPCB scenario-generation algorithm (introduced in Section 2.8) to provide the required scenarios for this experiment. Note that every scenario is unique and used only once in this analysis. Moreover, as a simplifying assumption, we consider a uniform probability of occurrence for all the scenarios ($\phi_v = 1/|\{v\}|, \forall v$).

The results of this experiment are presented in Fig. 11. Each box plot in this figure displays the distribution of the aggregator's profit (objective value of the optimization problem in SDPQ) for a fixed number of scenarios. In this case, the fluctuation of the profit stems from the variance of the underlying time series in each of the generated scenarios. The trend of the median values indicates that, with an increasing number of scenarios, the aggregator's expected profit tends to drop. We observed that solving the SDPQ with a higher number of scenarios, e.g., larger than 100, the median value falls below 100 ¢. In the formulated stochastic problem, regardless of the number of scenarios, the aggregator chooses a single set of prices for the users (see also (1a)). With an increasing number of scenarios, these prices are less tailored to each individual scenario and therefore the overall efficiency of the ORTP drops. Moreover, the aggregator's profit is more sensitive to the scenarios when the number of scenarios is lower. For instance, in the deterministic solution, i.e., $|\{v\}| = 1$, the profit of the aggregator varies between 104 and 382 ¢ (267% change) depending on the selected scenario. This range is reduced to 121 and 174 ¢ (43% change), when the number of scenarios is 47. Due to the considered uniform probability of scenarios, the impact of extreme scenarios reduces when the number of scenarios increases. This leads to a smaller spread of profit in the cases simulated with high numbers of scenarios.

Due to computational limitations, for the comparative analysis in Section 4, we solved the SDPQ with nine scenarios ($|\{v\}| = 9$). In Section 4.2, we present a sensitivity analysis and elaborate on the dependency of the computational efforts to solve the formulated problem on the numbers of users, optimization time steps, and scenarios.

[8] These cases are optimized using high performance computer Tegner PDC with 24 computational nodes and 32 threads [64].

4. Comparison of results

4.1. CW comparison

The results regarding the aggregator's profit, users' total costs, and the CW of the EC for the proposed ORTP tariff together with those derived from AP and RTP schemes are presented in Table 6 (the contents of this table are plotted in Appendix A.3). With the implementation of the ORTP, the CW of the EC has the highest value relative to the two other tariff strategies. In the setup in which only one flexible user interacts with the aggregator (Case study I), the RTP tariff performs as well as the ORTP tariff. In more complicated setups with multiple users, the ORTP tariff outperforms the RTP tariff. The AP tariff, the current pricing strategy for many small-scale electricity users in Germany, demonstrates the lowest CW value. This tariff does not contain any real-time signals relating to the scarcity or surplus of electricity (in the market or the EC). Note that we did not monetize the achieved grid relief by the ORTP in Case study III. In such a case, we would expect that the achieved CW in the ORTP tariff would outperform the benchmark tariffs by an even higher margin.

In all case studies, the aggregator's profit reveals the highest and lowest values for the ORTP and AP versions, respectively. However, the aggregator's profit in the benchmarks depends on the choice of the aggregator's margin. (Γ^{X}). Larger Γ^{X} values will lead to greater profits for the aggregator, which come at higher costs for the users. This will be a policy decision for the EC stakeholders as the aggregator's profit increases the EC's assets; these may be redistributed to users or invested.

4.2. Computational comparison

Table 7 compares the performance of the MBB algorithm and the benchmark algorithms introduced in Section 2.5 for the four case studies (the contents of this table are plotted in Appendix A.3). The model statistics and the number of discretization steps (k) in different cases under investigation are given in 8. We carried out the optimization for both the MILP and LP models on GAMS 25.1.3 platform using the CPLEX 12.8 solver. The case studies I–IV are optimized on a laptop with Intel Core i7-8650U CPU running at 1.90 GHz with eight nodes and 16 threads. Note that our algorithm does not use parallel computation and therefore, even though multiple processors were available, all the calculations were carried out on a single CPU node.

The optimal solution of SDPQ (the profit of the aggregator) depends substantially on the level of discretization (k); a larger number of discretization steps will converge closer to the optimal solution of the original problem in (1).

The results in Table 7 clearly show that the MBB algorithm outperforms the SBB algorithm (from [54]) and the MILP model, as it is able to reach a better objective value with fewer iterations and less computation time. These improvements increase in more complex cases. For example, in Case study IV, the MBB algorithm converges to an objective value, which is respectively 9.2% and 11% higher than those from the SBB algorithm and MILP model with 83.1% and 91.8% less solver execution time. This indicates the efficient performance of our proposed MBB algorithm, especially for solving large-scale problems.

A convergence plot of the proposed MBB and the benchmark SBB algorithms for Case study III is presented in Fig. 12. Starting with a lower value k, the MBB algorithm converges to the objective value of 76.49 after 768 iterations for the first time. After this step, the discretized prices are dynamically modified, and LB is set back to $-\infty$. After five more rounds, the algorithm converges to the objective value of 123.25 in iteration 2189. In contrast, with $k = 5$, the SBB

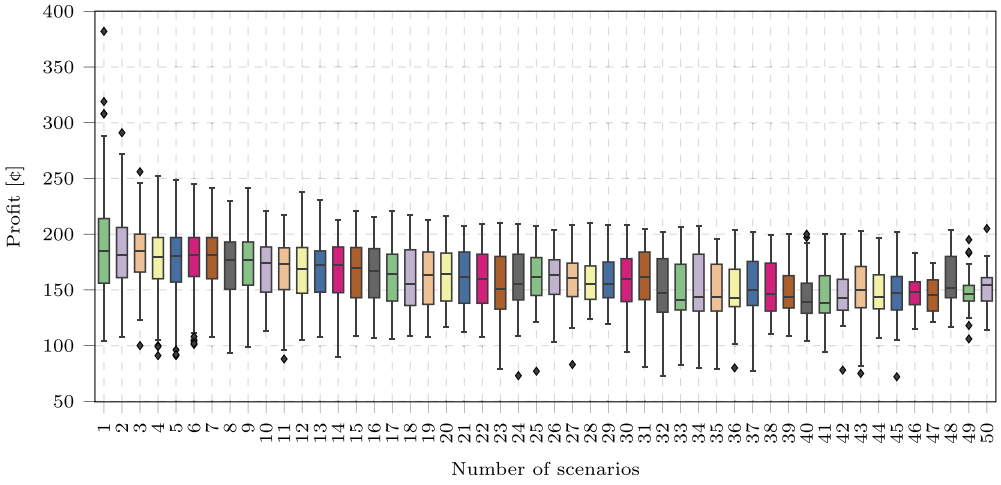

Fig. 11. Sensitivity analysis of the impact of the number of scenarios on the aggregator's profit in Case study IV. Box plots show the distribution of profit with the corresponding quartiles (25%, 50%, 75%).

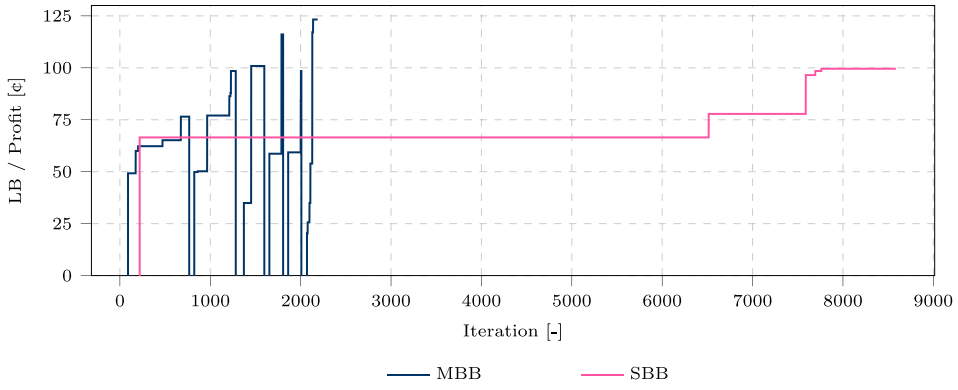

Fig. 12. Convergence plot of the benchmark SBB and MBB algorithms for Case study III. The LB values lower than zero are not shown in the figure.

Table 6
Comparison of aggregator's profit, users' costs and CW under different tariff strategies.

Tariff	Case study I			Case study II			Case study III			Case study IV		
	r [¢]	C' [¢]	CW [¢]	r [¢]	C' [¢]	CW [¢]	r [¢]	C' [¢]	CW [¢]	r [¢]	C' [¢]	CW [¢]
ORTP	**105.7**	**1.7**	**104**	**93.36**	**−13.31**	**106.67**	**99.6**	**52.3**	**47.3**	**181.1**	**−2.7**	**183.8**
AP	−14	2	−16	12.59	−0.67	13.26	4.3	199.9	−195.6	23.5	−31.3	54.8
RTP	18	−86	104	22.45	−84.22	106.67	28.4	338.6	−310.2	50.2	−56.1	106.3

Table 7
Comparison of the computational performance.

Case	Number of iterations [–]			Nodes explored [–]			CPU time [s]			Profit (r) [¢]		
	MILP	SBB	**MBB**	MILP	SBB	**MBB**	MILP	SBB	**MBB**	MILP	SBB	**MBB**
I	1226	306	**104**	203	296	**102**	5.12	0.69	**0.37**	105.75	105.75	**105.75**
II	70439	5959	**1701**	19945	5610	**1608**	35.39	18.22	**5.85**	93.36	91.17	**102.34**
III	876382	8586	**2188**	141848	7761	**2138**	347.2	26.83	**6.9**	99.55	99.55	**123.25**
IV	50227324	41254	**6086**	190145	30058	**4021**	10935	5270	**924.3**	181.08	184.18	**201.14**

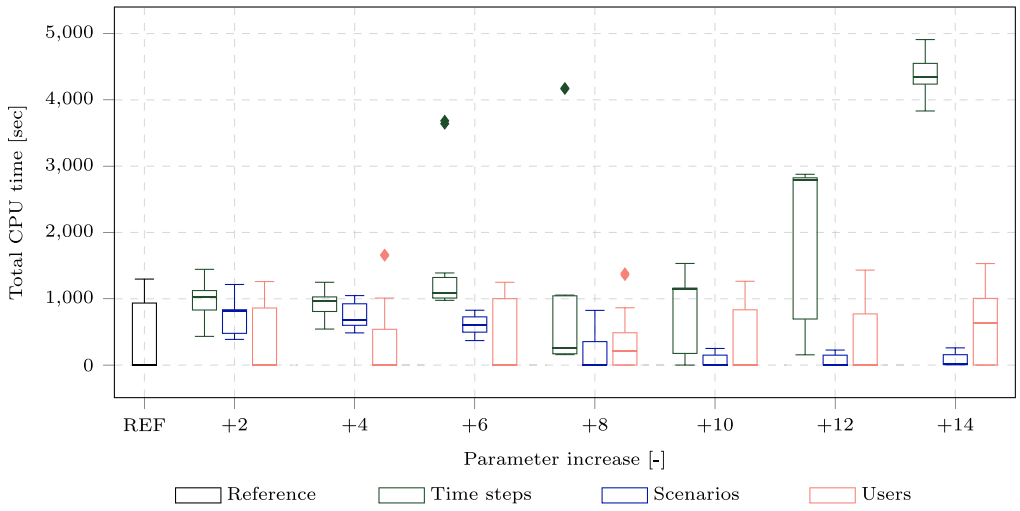

Fig. 13. Sensitivity analysis regarding the impact of optimization time steps, number of users, and scenarios on the computation time. The numbers on the x-axis indicate the increased value of the parameters under study relative to the reference case.

Table 8
Model statistics.

Case	Bin.	Con.	Const.	$\|k\|_{MILP}$	$\|k\|_{SBB}$	$\|k\|_{MBB}$
I	38	115	198	9	9	3
II	44	163	264	5	5	3
III	48	277	495	5	5	3
IV	819	8799	16035	4	4	3

Bin.: Number of binary variables. Con.: Number of continuous variables. Const.: Number of constraints.

algorithm, achieves the optimal value of 99.55 after 8587 iterations. This shows that a significant efficiency improvement is made by the MBB algorithm. Note that each round of optimization is finished, when the termination criteria (see Section 2.4) are fulfilled.

To assess the sensitivity of the computation effort to three key model parameters, i.e., number of optimization time-steps, users, and scenarios, we perform another simulation experiment. The starting point of our sensitivity analysis is a reference case, which is parameterized identically to Case III (i.e., with five time steps, one scenario, and two users). In three parallel analyses (one for each parameter), we increase the parameters and carry out more than 600 simulations with unique scenarios. The required CPU time for the simulated cases is presented in Fig. 13.[9] The x-axis in Fig. 13 shows the increased number of time steps, scenarios, and users (with the maximum value of 14) in each analysis.

The computation time of the reference case (black box in Fig. 13) varies between 0.6 and 1297 s. This fluctuation indicates a strong dependency of the computation effort to the input time series (electricity demand, generation, and market prices). The findings of the simulation experiment reveal that the required computation time rises significantly when prolonging the optimization period. Simulations with 19 time steps (14 steps more than REF) require an average computation time of 4370 s. In contrast, optimizing the formulated problem with a larger number of users does not increase the needed solution time substantially. When increasing the number of scenarios, we observed that stochastic optimizations with larger $|\{v\}|$ were solved faster than deterministic optimizations. For instance, the maximum recorded computation time for the cases with 13 and 15 scenarios (12 and 14 scenarios more than REF) is 226 and 259 s. These findings indicate that the proposed model scalable with respect to the number of scenarios and users in the EC. In contrast, increasing the optimization period above 14 time steps seem to have a strong impact on the required computation effort.

5. Discussion of limitations and implications for external validity

The results of our analysis demonstrate that the implementation of DR in ECs with the help of smart real-time pricing strategies can potentially lead to technical and economic benefits. Our evaluation did not assess the practical implementation of this pricing strategy. The following are pointers to future research needs.

Concerning the economic benefits of the proposed pricing strategy, a question arises about how the generated welfare is redistributed among the stakeholders; i.e., what are the financial incentives for the users to participate in this business model, rather than switching to another retailer. In this regard, the absence of competition among aggregators is a limitation of our model that should be addressed in future research. Moreover, the observed actor behavior in this analysis could be distorted by the addition of regulatory-induced charges to the electricity consumer price.[10] Expensive electricity consumer prices generally

[9] For this simulation experiment, we used the processor AMD EPYC 2.25 GHz and 16 GB memory from the recent KTH Dardel system [65].

[10] These regulatory-induced charges do not contain any time-varying signal and comprised more than 70% of the end-user electricity price in Germany in the year 2021.

incentivize a higher level of behind-the-meter self-consumption for the prosumagers [66]. Because we neglected the impact of these consumer-price components, future research should assess the adaptability of such real-time pricing schemes in different regulatory environments.

With an efficient operation, ECs can support the power network and enhance the integration of renewable energies. In this paper, we demonstrated that the ORTP strategy can incentivize an operation that contributes to power-grid relief. Quantifying the value of the delivered flexibility requires a more comprehensive study with the help of a distribution grid model. Along with these benefits, the establishment of ECs can arouse concerns regarding inefficient investments and increasing overall energy-system costs. For instance, if sharing the electricity across the EC reduces the revenues of the distribution grid, raising the grid charges for other consumers is likely. This effect may exacerbate inequalities and incentivize local self-consumption even further. In this case, solutions such as distribution-network tariffs are suggested in the literature [67]. Therefore, further studies are required concerning the impact of the (collective) self-consumption in ECs on the larger energy system. A useful approach for such analysis is the coupling of models with different perspectives (e.g., local and national perspectives) [68].

Regarding the technical implementation, this paper assumes that the bidirectional communication infrastructure and the required measuring and control equipment for an efficient and secure transmission of data is available in the EC. Therefore, we have neglected the investment costs in our calculations. For the case of Germany, users need to be equipped with smart-meter gateways, which are devices that automatically communicate measurements from connected smart meters to external market participants; these allow them to send incentives or commands for load adjustments to local control boxes such as energy-management systems [69]. While a general advantage of the price-based DR measures is respecting users' privacy [8], a limitation of the single-level reduction approach in solving bilevel optimization problems (compared to distributed algorithms such as [35]) is the necessity for sharing information about users with the aggregator. The technical evaluation of the technologies and algorithms that enable an efficient and secure transmission of the necessary data is part of another field of research [70]. Concerning our proposed methodology, we demonstrated that the presented modeling approach and solving technique can significantly contribute to a more effective solution of the bilevel problem when compared to the benchmark solving approaches. Real-world applications, however, can lead to optimization problems with longer durations and more heterogeneous users. Improving the performance of the proposed methodology to satisfy real-world-scale problems should be the focus of future research. In this context, one direction to improving the scalability potential of the algorithm is the simultaneous evaluation of the created branches on multiple processors using parallel computing [71].

6. Conclusion

The expansion of distributed electricity generation and storage potential poses challenges for the efficient technical and economic operation of the power system. Smart-grid infrastructure has opened the door to many innovative DR business models that can contribute to meeting these challenges while creating financial benefits for the participating actors. In this context, we have proposed an ORTP methodology for a profit-maximizing community-owned aggregator in an EC, that is not isolated from the wholesale market. In our model, the aggregator trades bilaterally with users in the EC (e.g., prosumagers and electric vehicles) while coping with restrictions regarding the maximum available line capacity behind the point of common coupling. Moreover, the stochastic formulation of the problem provides a solution for the aggregator to deal with uncertainties regarding the wholesale market prices as well as users' electricity demand and generation. The required representative scenarios for these sources of uncertainty are produced by developing a multi-parameter cluster-based scenario-generation approach. To capture the hierarchical nature of the decision-making process in the considered setup, the interplay between the users and the aggregator is formulated as a bilevel optimization problem. To solve the resulting problem efficiently, we reformulated the original stochastic bilevel program as a stochastic disjunctive program and proposed a novel MBB algorithm that applies a linear quasi-relaxation approach and a dynamic partitioning technique. We assessed the effectiveness of our proposed methodology in four cases studies.

Our results show that the derived ORTP leads to higher community welfare for the EC. Furthermore, if necessary, the ORTP can provide useful grid services by creating incentives to offset the EC's demand and supply locally. The comparison of the ORTP with the average pricing strategy (with no time-varying component) shows a significant improvement in all studied cases. However, the effectiveness of the ORTP against a simple real-time pricing strategy (including only signals from the wholesale market) becomes evident when the diversity of users increases. Moreover, our proposed algorithm outperforms the benchmark algorithms both in computational performance and community welfare. These enhancements were found to be more substantial in the large-scale case studies. There are two major drivers for the achieved improvements: first, by applying the quasi-relaxation approach a large number of binary variables are eliminated; second, the implemented dynamic partitioning technique disentangles the optimization results from the disjunctive parameters. Our simulation experiments show that the computational effort is sensitive to the number of optimization time steps. In contrast, the proposed model is observed to be scalable in terms of the number of users and scenarios. One direction of future studies includes assessing the impact of ECs on the German electricity market. Another objective of the subsequent studies will be the further development and enhancement of the proposed EC model and the solution algorithm.

Acknowledgements

The authors would like to thank Niklas Wulff for his support in preparing the electric vehicle data and the anonymous reviewers for their helpful comments on earlier versions of this work.

CRediT authorship contribution statement

Seyedfarzad Sarfarazi: Conceptualization, Methodology, Formal analysis, Writing – original draft, Writing – review & editing, Visualization, Project administration. **Saeed Mohammadi:** Methodology, Formal analysis, Writing – review & editing, Visualization. **Dina Khastieva:** Methodology. **Mohammad Reza Hesamzadeh:** Supervision, Writing – review & editing. **Valentin Bertsch:** Supervision, Writing – review & editing. **Derek Bunn:** Writing – review & editing.

Declaration of competing interest

The authors declare that they have no known competing financial interests or personal relationships that could have appeared to influence the work reported in this paper.

Data availability

The authors do not have permission to share data.

Appendix

A.1. Proof of Proposition 1

We start with the objective on the left-hand side of (2), which is defined in (29a). In (29), $\{p_t^S, p_t^B\}$ and χ are sets of decision variables for the user and the aggregator, respectively and $\chi = \{e_{itv}^S, e_{itv}^B, a_{itv}, z_{itv}^C, z_{itv}^D\}$. The expression $-\sum_{iv}\phi_v C_{iv}(\chi)$ is not a function of p_t^S and p_t^B. Therefore, it can be added to the objective function in (29a) without changing the optimal solution, i.e., (29a) and (29b) are equivalent. From (1), the expression $r(p_t^S, p_t^B)$ can be replaced with its equivalent $\sum_{itv}\phi_v r_{itv}(p_t^S, p_t^B)$, as done in (29c). Then, we can extract ϕ_v in (29d); this has the term $(r_{itv}(p_t^S, p_t^B) - C_{iv}(\chi))$, which is the CW. The terms $r(p_t^S, p_t^B)$ and $-C_{iv}(\chi)$ indicate profit of the aggregator and user i, respectively. CW can be defined as a summation of revenue of all the participants in the EC (users and the aggregator). Therefore, CW $= r_{itv}(p_t^S, p_t^B) - c_{itv}(\chi)$. Note that ϕ_v is a fixed parameter that does not change with the decision variables.

$$\underset{p_t^S, p_t^B}{\text{Maximize}}\ r(p_t^S, p_t^B) \equiv \tag{29a}$$

$$\underset{p_t^S, p_t^B}{\text{Maximize}}\ \left(r(p_t^S, p_t^B) - \sum_{iv}\phi_v C_{iv}(\chi)\right) \equiv \tag{29b}$$

$$\underset{p_t^S, p_t^B}{\text{Maximize}}\ \left(\sum_{itv}\phi_v r_{itv}(p_t^S, p_t^B) - \sum_{iv}\phi_v C_{iv}(\chi)\right) \equiv \tag{29c}$$

$$\underset{p_t^S, p_t^B}{\text{Maximize}}\ \sum_{itv}\phi_v \underbrace{\left(r_{itv}(p_t^S, p_t^B) - C_{iv}(\chi)\right)}_{=\text{CW}} \tag{29d}$$

We have started from the left-side of (2) and demonstrated that it is equivalent to the right-side of (2), which is CW. This shows that solving (1) is equivalent to maximizing the CW, as stated in (2). □

A.2. EV parameterization

The optimization of the charging schedule for EVs requires a deliberate consideration of their mobility pattern. Assuming a price-inelastic transport demand, we should know when the EV is available for charging/discharging from/to the grid (the battery storage of the prosumager is connected to the grid the whole time) and what the electricity consumption of the EV is. Due to a lack of suitable empirical open-source data, in this work, the VencoPy tool was deployed to derive these data. VencoPy uses data from the German national travel survey [61] and aims to estimate future electric vehicle fleet charging flexibility [60]. In the first step (trip diary building), the individual trips are consolidated into a user-specific travel diary. In this step, the driven distance and the travel purpose (e.g., shopping, returning home, etc.) are allocated to their respective hour and merged into the daily travel diaries. In the next step, using a basic charging infrastructure model, the charging availability is allocated through a binary True–False mapping of the respective trip purposes. Since we focus on the technical load-shifting potential, and due to lack of sufficient data, user behavior (e.g., state-of-charge dependent plugging decisions) is disregarded. The result of the charging-availability allocation is a binary grid connection profile that describes whether the EV is connected to the grid at a given hour. To calculate the electricity flow from the battery to the electric motor, the driven distance is multiplied by an assumed average specific electricity consumption in 100 kWh/100 km. The two resulting profiles, together with the technical parameters of the storage, are then passed to the EC model. Fig. 14 gives an overview of the described steps to calculate the EV load and availability profiles. The interested reader can refer to [60] for a more detailed explanation of the internal calculations of VencoPy.

A.3. Visualization of the comparative results

In this section, we visualize the comparative results presented in Section 4. Fig. 15 shows the achieved community welfare with ORTP compared to the benchmark tariffs AP and RTP. Fig. 16 compares the computational performance of the MBB with the benchmark approaches SBB and MILP. Figs. 15 and 16 respectively correspond to Tables 6 and 7.

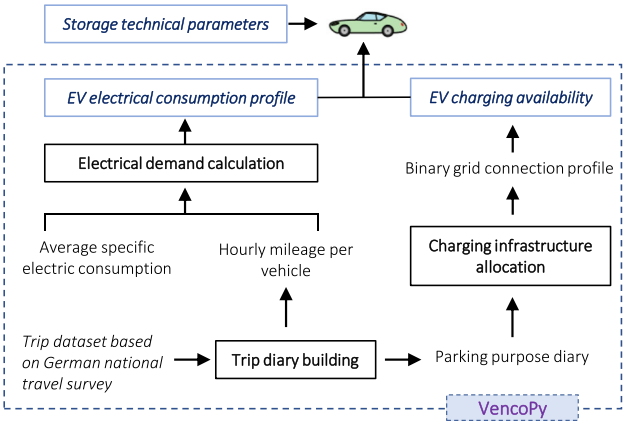

Fig. 14. Data preparation using the VencoPy tool.

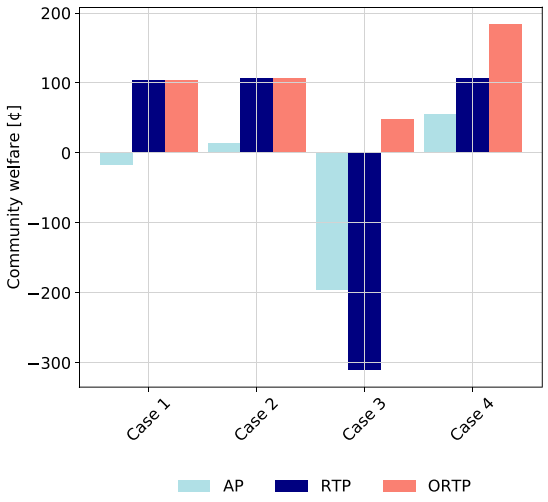

Fig. 15. Community welfare for the studied tariffs in different case studies.

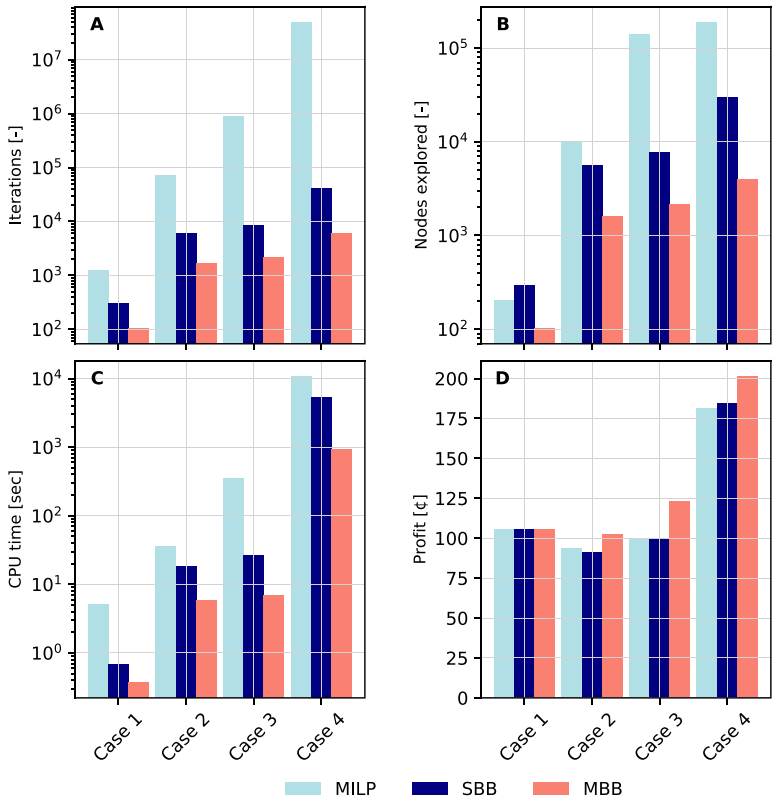

Fig. 16. Computational performance of the benchmark MILP approach compared to the SBB and MBB algorithms. A: Number of iterations. B: Number of explored nodes. C: CPU time. D: Aggregator's profit (r).

References

[1] Schill W-P, Zerrahn A, Kunz F. Prosumage of solar electricity: pros, cons, and the system perspective. Economics of Energy & Environmental Policy 2017;6(1):7–32. http://dx.doi.org/10.5547/2160-5890.6.1.wsch.

[2] Bertsch V, Geldermann J, Lühn T. What drives the profitability of household PV investments, self-consumption and self-sufficiency? Appl Energy 2017;204:1–15. http://dx.doi.org/10.1016/j.apenergy.2017.06.055.

[3] Hoppmann J, Volland J, Schmidt TS, Hoffmann VH. The economic viability of battery storage for residential solar photovoltaic systems–A review and a simulation model. Renew Sustain Energy Rev 2014;39:1101–18. http://dx.doi.org/10.1016/j.rser.2014.07.068.

[4] Ajanovic A, Haas R. On the economics and the future prospects of battery electric vehicles. Greenhouse Gases: Sci Technol 2020;10(6):1151–64. http://dx.doi.org/10.1002/ghg.1985.

[5] Klein M, Ziade A, De Vries L. Aligning prosumers with the electricity wholesale market–The impact of time-varying price signals and fixed network charges on solar self-consumption. Energy Policy 2019;134:110901. http://dx.doi.org/10.1016/j.enpol.2019.110901.

[6] Kakran S, Chanana S. Smart operations of smart grids integrated with distributed generation: A review. Renew Sustain Energy Rev 2018;81:524–35.

[7] Haider HT, See OH, Elmenreich W. A review of residential demand response of smart grid. Renew Sustain Energy Rev 2016;59:166–78. http://dx.doi.org/10.1016/j.rser.2016.01.016.

[8] Xiao Y. Communication and networking in smart grids. CRC Press; 2012, http://dx.doi.org/10.1201/b11897.

[9] Yan X, Ozturk Y, Hu Z, Song Y. A review on price-driven residential demand response. Renew Sustain Energy Rev 2018;96:411–9. http://dx.doi.org/10.1016/j.rser.2018.08.003.

[10] Soeiro S, Dias MF. Renewable energy community and the European energy market: main motivations. Heliyon 2020;6(7):e04511. http://dx.doi.org/10.1016/j.heliyon.2020.e04511.

[11] Caramizaru A, Uihlein A. Energy communities: an overview of energy and social innovation. vol. 30083, Publications Office of the European Union Luxembourg; 2020, http://dx.doi.org/10.2760/180576.

[12] Hogan WW. Time-of-use rates and real-time prices. 2014, https://hepg.hks.harvard.edu/files/hepg/files/hogan_tou_rtp_newark_082314.pdf, John F. Kennedy School of Government, Harvard University.

[13] Freier J, von Loessl V. Dynamic electricity tariffs: Designing reasonable pricing schemes for private households. Energy Econ 2022;112:106146. http://dx.doi.org/10.1016/j.eneco.2022.106146.

[14] Anees A, Dillon T, Wallis S, Chen Y-PP. Optimization of day-ahead and real-time prices for smart home community. Int J Electr Power Energy Syst 2021;124:106403. http://dx.doi.org/10.1016/j.ijepes.2020.106403.

[15] Lu Q, Guo Q, Zeng W. Optimization scheduling of home appliances in smart home: A model based on a niche technology with sharing mechanism. Int J Electr Power Energy Syst 2022;141:108126. http://dx.doi.org/10.1016/j.ijepes.2022.108126.

[16] McKenna K, Keane A. Residential load modeling of price-based demand response for network impact studies. IEEE Trans Smart Grid 2015;7(5):2285–94. http://dx.doi.org/10.1109/TSG.2015.2437451.

[17] Mohsenian-Rad A-H, Leon-Garcia A. Optimal residential load control with price prediction in real-time electricity pricing environments. IEEE Trans Smart Grid 2010;1(2):120–33. http://dx.doi.org/10.1109/TSG.2010.2055903.

[18] Atzeni I, Ordóñez LG, Scutari G, Palomar DP, Fonollosa JR. Noncooperative and cooperative optimization of distributed energy generation and storage in the demand-side of the smart grid. IEEE Trans Signal Process 2013;61(10):2454–72. http://dx.doi.org/10.1109/TSP.2013.2248002.

[19] Tushar W, Saha TK, Yuen C, Smith D, Poor HV. Peer-to-peer trading in electricity networks: An overview. IEEE Trans Smart Grid 2020;11(4):3185–200. http://dx.doi.org/10.1109/TSG.2020.2969657.

[20] Cui S, Wang Y-W, Xiao J-W. Peer-to-peer energy sharing among smart energy buildings by distributed transaction. IEEE Trans Smart Grid 2019;10(6):6491–501. http://dx.doi.org/10.1109/TSG.2019.2906059.

[21] Cui S, Wang Y-W, Shi Y, Xiao J-W. A new and fair peer-to-peer energy sharing framework for energy buildings. IEEE Trans Smart Grid 2020;11(5):3817–26. http://dx.doi.org/10.1109/TSG.2020.2986337.

[22] Mengelkamp E, Bose S, Kremers E, Eberbach J, Hoffmann B, Weinhardt C. Increasing the efficiency of local energy markets through residential demand response. Energy Inform 2018;1(1):1–18. http://dx.doi.org/10.1186/s42162-018-0017-3.

[23] Henggeler Antunes C, Alves MJ, Ecer B. Bilevel optimization to deal with demand response in power grids: models, methods and challenges. Top 2020;28(3):814–42. http://dx.doi.org/10.1007/s11750-020-00573-y.

[24] Li H, Wan Z, He H. Real-time residential demand response. IEEE Trans Smart Grid 2020;11(5):4144–54. http://dx.doi.org/10.1109/TSG.2020.2978061.

[25] Saad W, Han Z, Poor HV, Basar T. Game-theoretic methods for the smart grid: An overview of microgrid systems, demand-side management, and smart grid communications. IEEE Signal Process Mag 2012;29(5):86–105. http://dx.doi.org/10.1109/MSP.2012.2186410.

[26] Rajabi A, Li L, Zhang J, Zhu J. Aggregation of small loads for demand response programs—Implementation and challenges: A review. In: 2017 IEEE international conference on environment and electrical engineering and 2017 IEEE industrial and commercial power systems Europe. IEEE; 2017, p. 1–6. http://dx.doi.org/10.1109/EEEIC.2017.7977631.
[27] Rashidizadeh-Kermani H, Vahedipour-Dahraie M, Najafi HR, Anvari-Moghaddam A, Guerrero JM. A stochastic bi-level scheduling approach for the participation of EV aggregators in competitive electricity markets. Appl Sci 2017;7(10):1100. http://dx.doi.org/10.3390/app7101100.
[28] Rashidizadeh-Kermani H, Vahedipour-Dahraie M, Shafie-khah M, Catalão JP. Stochastic programming model for scheduling demand response aggregators considering uncertain market prices and demands. Int J Electr Power Energy Syst 2019;113:528–38. http://dx.doi.org/10.1016/j.ijepes.2019.05.072.
[29] Liu N, Yu X, Wang C, Wang J. Energy sharing management for microgrids with PV prosumers: A Stackelberg game approach. IEEE Trans Ind Inf 2017;13(3):1088–98. http://dx.doi.org/10.1109/TII.2017.2654302.
[30] Yu M, Hong SH. A real-time demand-response algorithm for smart grids: A stackelberg game approach. IEEE Trans Smart Grid 2015;7(2):879–88. http://dx.doi.org/10.1109/TSG.2015.2413813.
[31] Besançon M, Anjos MF, Brotcorne L, Gomez-Herrera JA. A bilevel approach for optimal price-setting of time-and-level-of-use tariffs. IEEE Trans Smart Grid 2020;11(6):5462–5. http://dx.doi.org/10.1109/TSG.2020.3000651.
[32] Liu N, Cheng M, Yu X, Zhong J, Lei J. Energy-sharing provider for PV prosumer clusters: A hybrid approach using stochastic programming and stackelberg game. IEEE Trans Ind Electron 2018;65(8):6740–50. http://dx.doi.org/10.1109/TIE.2018.2793181.
[33] Mediwaththe CP, Stephens ER, Smith DB, Mahanti A. Competitive energy trading framework for demand-side management in neighborhood area networks. IEEE Trans Smart Grid 2017;9(5):4313–22. http://dx.doi.org/10.1109/TSG.2017.2654517.
[34] Mediwaththe CP, Shaw M, Halgamuge S, Smith DB, Scott P. An incentive-compatible energy trading framework for neighborhood area networks with shared energy storage. IEEE Trans Sustain Energy 2019;11(1):467–76. http://dx.doi.org/10.1109/TSTE.2019.2895387.
[35] Sarfarazi S, Deissenroth-Uhrig M, Bertsch V. Aggregation of households in community energy systems: An analysis from actors' and market perspectives. Energies 2020;13(19):5154. http://dx.doi.org/10.3390/en13195154.
[36] Fioriti D, Poli D, Frangioni A. A bi-level formulation to help aggregators size energy communities: a proposal for virtual and physical closed distribution systems. In: 2021 IEEE international conference on environment and electrical engineering and 2021 IEEE industrial and commercial power systems Europe. IEEE; 2021, p. 1–6. http://dx.doi.org/10.1109/EEEIC/ICPSEurope51590.2021.9584536.
[37] Liu W, Chen S, Hou Y, Yang Z. Optimal reserve management of electric vehicle aggregator: Discrete bilevel optimization model and exact algorithm. IEEE Trans Smart Grid 2021;12(5):4003–15. http://dx.doi.org/10.1109/TSG.2021.3075710.
[38] Rashidizadeh-Kermani H, Vahedipour-Dahraie M, Shafie-Khah M, Siano P. A regret-based stochastic bi-level framework for scheduling of DR aggregator under uncertainties. IEEE Trans Smart Grid 2020;11(4):3171–84. http://dx.doi.org/10.1109/TSG.2020.2968963.
[39] Samadi P, Mohsenian-Rad A-H, Schober R, Wong VW, Jatskevich J. Optimal real-time pricing algorithm based on utility maximization for smart grid. In: 2010 First IEEE international conference on smart grid communications. IEEE; 2010, p. 415–20. http://dx.doi.org/10.1109/SMARTGRID.2010.5622077.
[40] Kovacevic RM, Vo N-V, Haunschmied J. Bilevel approaches for distributed DSM using internal individualized prices. In: 2017 IEEE internatonal conference on smart grid communications. IEEE; 2017, p. 521–6. http://dx.doi.org/10.1109/SmartGridComm.2017.8340709.
[41] ALSalloum H, ELMasri A, Merghem-Boulahia L, Rahim R. Demand side management in smart grids: A stackelberg multi period multi provider game. In: 2018 9th IFIP international conference on new technologies, mobility and security. IEEE; 2018, p. 1–5. http://dx.doi.org/10.1109/NTMS.2018.8328687.
[42] Meng F-L, Zeng X-J. An optimal real-time pricing for demand-side management: A stackelberg game and genetic algorithm approach. In: 2014 International joint conference on neural networks. IEEE; 2014, p. 1703–10. http://dx.doi.org/10.1109/IJCNN.2014.6889608.
[43] Meng F-L, Zeng X-J. A bilevel optimization approach to demand response management for the smart grid. In: 2016 IEEE congress on evolutionary computation. IEEE; 2016, p. 287–94. http://dx.doi.org/10.1109/CEC.2016.7743807.
[44] Mediwaththe CP, Smith DB. Game-theoretic demand-side management robust to non-ideal consumer behavior in smart grid. In: 2016 IEEE 25th international symposium on industrial electronics. IEEE; 2016, p. 702–7. http://dx.doi.org/10.1109/ISIE.2016.7744975.
[45] Mu L, Yu N, Huang H, Du H, Jia X. Distributed real-time pricing scheme for local power supplier in smart community. In: 2016 IEEE 22nd international conference on parallel and distributed systems. IEEE; 2016, p. 40–7. http://dx.doi.org/10.1109/ICPADS.2016.0015.
[46] Latifi M, Khalili A, Rastegarnia A, Sanei S. Fully distributed demand response using the adaptive diffusion–Stackelberg algorithm. IEEE Trans Ind Inf 2017;13(5):2291–301. http://dx.doi.org/10.1109/TII.2017.2703132.
[47] Ben-Ayed O, Blair CE. Computational difficulties of bilevel linear programming. Oper Res 1990;38(3):556–60. http://dx.doi.org/10.1287/opre.38.3.556.
[48] Sinha A, Malo P, Deb K. A review on bilevel optimization: From classical to evolutionary approaches and applications. IEEE Trans Evol Comput 2018;22(2):276–95. http://dx.doi.org/10.1109/TEVC.2017.2712906.
[49] Liu N, Yu X, Wang C, Li C, Ma L, Lei J. Energy-sharing model with price-based demand response for microgrids of peer-to-peer prosumers. IEEE Trans Power Syst 2017;32(5):3569–83. http://dx.doi.org/10.1109/TPWRS.2017.2649558.
[50] Meng F-L, Zeng X-J. A profit maximization approach to demand response management with customers behavior learning in smart grid. IEEE Trans Smart Grid 2015;7(3):1516–29. http://dx.doi.org/10.1109/TSG.2015.2462083.
[51] Angelo JS, Barbosa HJ. A study on the use of heuristics to solve a bilevel programming problem. Int Trans Oper Res 2015;22(5):861–82. http://dx.doi.org/10.1111/itor.12153.
[52] Colson B, Marcotte P, Savard G. An overview of bilevel optimization. Ann Oper Res 2007;153(1):235–56. http://dx.doi.org/10.1007/s10479-007-0176-2.
[53] Quashie M, Bouffard F, Marnay C, Jassim R, Joós G. On bilevel planning of advanced microgrids. Int J Electr Power Energy Syst 2018;96:422–31. http://dx.doi.org/10.1016/j.ijepes.2017.10.019.
[54] Tómasson E, Hesamzadeh MR, Wolak FA. Optimal offer-bid strategy of an energy storage portfolio: A linear quasi-relaxation approach. Appl Energy 2020;260:114251. http://dx.doi.org/10.1016/j.apenergy.2019.114251.
[55] Bollapragada S, Ghattas O, Hooker JN. Optimal design of truss structures by logic-based branch and cut. Oper Res 2001;49(1):42–51. http://dx.doi.org/10.1287/opre.49.1.42.11196.
[56] Rossetto N, Verde SF, Bauwens T. A taxonomy of energy communities in liberalized energy systems. In: Energy communities. Elsevier; 2022, p. 3–23. http://dx.doi.org/10.1016/B978-0-323-91135-1.00004-3.
[57] Bard JF. Practical bilevel optimization: algorithms and applications. Springer New York, NY; 1998, http://dx.doi.org/10.1007/978-1-4757-2836-1.
[58] Gupta OK, Ravindran A. Branch and bound experiments in convex nonlinear integer programming. Manage Sci 1985;31(12):1533–46. http://dx.doi.org/10.1287/mnsc.31.12.1533.
[59] Tjaden T, Bergner J, Weniger J, Quaschning V, Solarspeichersysteme F. Repräsentative elektrische Lastprofile für Wohngebäude in Deutschland auf 1-sekündiger Datenbasis. Hochschule für Technik und Wirtschaft (HTW) Berlin 2015. downloaded: 2021-01-10.
[60] Wulff N, Miorelli F, Gils HC, Jochem P. Vehicle energy consumption in Python (VencoPy): Presenting and demonstrating an open-source tool to calculate electric vehicle charging flexibility. Energies 2021;14(14). http://dx.doi.org/10.3390/en14144349.
[61] Nobis C, Kuhnimhof T. Mobilität in deutschland- mid: Ergebnisbericht. 2018, https://elib.dlr.de/125879/.
[62] Data OPS. Data package time series. 2020, http://dx.doi.org/10.25832/time_series/2020-10-06.
[63] Rousseeuw PJ. Silhouettes: A graphical aid to the interpretation and validation of cluster analysis. J Comput Appl Math 1987;20:53–65. http://dx.doi.org/10.1016/0377-0427(87)90125-7.
[64] KTH Royal Institute of Technology. Tegner system in PDC Center for High Performance Computing. 2021, URL https://www.pdc.kth.se/hpc-services/computing-systems/tegner-1.737437.
[65] KTH Royal Institute of Technology. Dardel system in PDC Center for High Performance Computing. 2022, URL https://www.pdc.kth.se/hpc-services/computing-systems/about-dardel-1.1053338.
[66] Günther C, Schill W-P, Zerrahn A. Prosumage of solar electricity: Tariff design, capacity investments, and power sector effects. Energy Policy 2021;152:112168. http://dx.doi.org/10.1016/j.enpol.2021.112168.
[67] Biggar D, Hesamzadeh MR. Energy communities: challenges for regulators and policymakers. In: Energy communities. Elsevier; 2022, p. 131–49. http://dx.doi.org/10.1016/B978-0-323-91135-1.00002-X.
[68] Cao K-K, Haas J, Sperber E, Sasanpour S, Sarfarazi S, Pregger T, Alaya O, Lens H, Drauz SR, Kneiske TM. Bridging granularity gaps to decarbonize large-scale energy systems—The case of power system planning. Energy Sci Eng 2021;9(8):1052–60. http://dx.doi.org/10.1002/ese3.891.
[69] Förderer K, Lösch M, Növer R, Ronczka M, Schmeck H. Smart meter gateways: Options for a BSI-compliant integration of energy management systems. Appl Sci 2019;9(8):1634. http://dx.doi.org/10.3390/app9081634.
[70] Kroener N, Förderer K, Lösch M, Schmeck H. State-of-the-art integration of decentralized energy management systems into the German smart meter gateway infrastructure. Appl Sci 2020;10(11):3665. http://dx.doi.org/10.3390/app10113665.
[71] Bader DA, Hart WE, Phillips CA. Parallel algorithm design for branch and bound. In: Tutorials on emerging methodologies and applications in operations research. Springer; 2005, p. 5–1–5–44. http://dx.doi.org/10.1007/0-387-22827-6_5.